

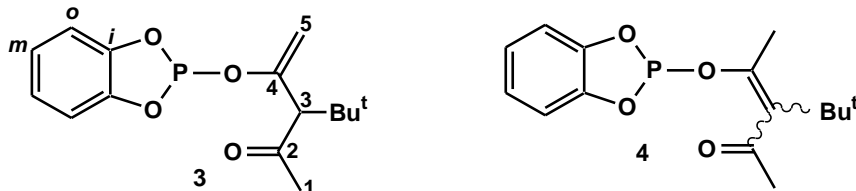
The reaction of 4-(1,3,2-benzodioxaphosphol-2-yloxy)-3-*tert*-butylpent-4-en-2-one with hexafluoroacetone

Vladimir F. Mironov, Tamara A. Baronova, Mudaris N. Dimukhametov and Igor A. Litvinov

Table of contents

General remarks	S2
Syntheses and characterization of compounds 3 and 5	S2
Figure S1. Geometry of molecule 6 in the crystal.	S4
Table S1. Bond lengths in the molecule of compound (5).	S5
Table S2. Bond angles in the molecule of compound (5).	S5
Table S3. Torsion angles in the molecule of compound (5).	S6
Figure S2. $^{31}\text{P}\{-^1\text{H}\}$ NMR spectrum of phospholes 3,4 mixture (procedure A).	S7
Figure S3. $^{31}\text{P}\{-^1\text{H}\}$ NMR spectrum of phosphole 3 (procedure B).	S8
Figure S4. ^1H NMR spectrum (400.0 MHz, CDCl_3 , 25°C) of phosphole (3).	S9
Figure S5. $^{13}\text{C}\{-^1\text{H}\}$ NMR spectrum (100.6 MHz, CDCl_3 , 25°C) of phosphole (3).	S10
Figure S6. ^{13}C NMR spectrum (100.6 MHz, CDCl_3 , 25°C) of phosphole (3).	S11
Figure S7. High-field region of ^{13}C NMR spectrum of phosphole (3).	S12
Figure S8. ^{13}C and $^{13}\text{C}\{-^1\text{H}\}$ NMR spectra (100.6 MHz, CDCl_3 , 25°C) of phosphole (3).	S13
Figure S9. The fragments of ^{13}C and $^{13}\text{C}\{-^1\text{H}\}$ NMR spectra of phosphole (3).	S14
Figure S10. The low-field fragments of ^{13}C and $^{13}\text{C}\{-^1\text{H}\}$ NMR spectra of phosphole (3).	S15
Figure S11. The high-field fragments of ^{13}C and $^{13}\text{C}\{-^1\text{H}\}$ NMR spectra phosphole (3).	S16
Figure S12. $^{31}\text{P}\{-^1\text{H}\}$ NMR spectrum of phosphoranes (5, 6) mixture.	S17
Figure S13. ^{31}P and $^{31}\text{P}\{-^1\text{H}\}$ NMR spectra of phosphoranes (5, 6) mixture.	S18
Figure S14. ^1H NMR spectrum of phosphoranes (5, 6) mixture.	S19
Figure S15. ^1H NMR spectra of phosphoranes (5, 6) mixture (blue) and phosphorane (6).	S20
Figure S16. ^{19}F NMR spectrum of phosphoranes (5, 6) mixture.	S21
Figure S17. $^{31}\text{P}\{-^1\text{H}\}$ NMR spectrum (162.0 MHz, CDCl_3 , 25°C) of phosphorane (6).	S22
Figure S18. ^1H NMR spectrum (400.0 MHz, CDCl_3 , 25°C) of phosphorane (6).	S23
Figure S19. ^{19}F NMR spectrum (386.5 MHz, CDCl_3 , 25°C) of phosphorane (6).	S24
Figure S20. ^{13}C and $^{13}\text{C}\{-^1\text{H}\}$ NMR spectra (100.6 MHz, CDCl_3 , 25°C) of phosphorane (6).	S25
Figure S21. High-field regions of ^{13}C and $^{13}\text{C}\{-^1\text{H}\}$ NMR spectra of phosphorane (6).	S26
Figure S22. C^3 , C^4 and C^7 region of ^{13}C and $^{13}\text{C}\{-^1\text{H}\}$ NMR spectra of phosphorane (6).	S27
Figure S23. C^9 , C^{12} and C^5 regions of ^{13}C and $^{13}\text{C}\{-^1\text{H}\}$ NMR spectra of phosphorane (6).	S28
Figure S24. Aromatic and CF_3 region of ^{13}C and $^{13}\text{C}\{-^1\text{H}\}$ NMR of phosphorane (6).	S29
Figure S25. CF_3 -groups region of ^{13}C and $^{13}\text{C}\{-^1\text{H}\}$ NMR spectra of phosphorane (6).	S30
Figure S26. Low-field region of ^{13}C and $^{13}\text{C}\{-^1\text{H}\}$ NMR spectra of phosphorane (6).	S31
Figure S27. $^{13}\text{C}\{-^1\text{H}\}$ and ^{13}C -dept NMR spectra of phosphorane (6).	S32
Figure S28. $^{13}\text{C}\{-^1\text{H}\}$ NMR spectrum (100.6 MHz, CDCl_3 , 25°C) of phosphorane (6).	S33
Figure S29. Aromatic and CF_3 region of $^{13}\text{C}\{-^1\text{H}\}$ NMR of phosphorane (6).	S34
Figure S30. ^{13}C NMR spectrum (100.6 MHz, CDCl_3 , 25°C) of phosphorane (6).	S35
Figure S31. C^9 and C^{12} -atoms region of ^{13}C NMR spectrum of phosphorane (6).	S36
Figure S32. Aromatic and CF_3 region of ^{13}C NMR spectrum of phosphorane (6).	S37
Figure S33. High-field region of ^{13}C NMR spectrum of phosphorane (6).	S38
Figure S34. IR Spectrum (Nujol) of phosphole (3).	S39
Figure S35. IR Spectrum (Nujol) of phosphorane (6).	S40

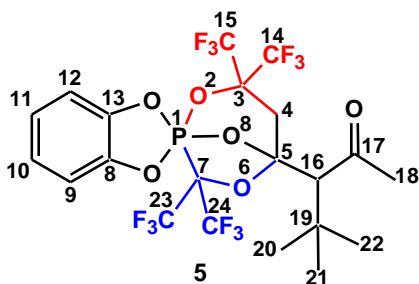
General remarks. NMR spectra were recorded using a 400 MHz spectrometer (400 MHz, ^1H ; 162.0 MHz, ^{31}P ; 376.3 MHz, ^{19}F ; 100.6 MHz, ^{13}C) at 25 °C in CDCl_3 , chemical shifts were measured relative to the signals of the solvent. High-resolution mass spectra (HRMS) were measured in EI mode with magnetic mass analyzers. Elemental analysis was performed on EuroVector-3000 instrument (C, H, N) or manually by pyrolysis in an oxygen stream (P).



4-(1,3,2-Benzodioxaphosphol-2-yl)oxy-3-tert-butylpent-4-en-2-one 3. Method A. In a three-necked 100 ml flask equipped with a stirrer, a reflux condenser, and an inlet for argon, there were placed benzene (100 ml), 3-tert-butylacetylacetone **1** (12.4 g, 79 mmol), triethylamine (12.2 ml, 87 mmol), chlorotrimethylsilane (3.5 ml, 28 mmol) and 2-chlorobenzo-1,3,2-dioxaphosphole **2** (13.9 g, 79 mmol). The mixture was heated (80 °C) for 64 hours, then cooled, the precipitate was filtered off, the filtrate was concentrated on a rotary evaporator, the residue was diluted with pentane (50 ml) and kept at 4 °C in a refrigerator for 12 hours. The precipitate formed was filtered off, the filtrate was concentrated on a rotary evaporator, and the residue was distilled in vacuum. Yield of the mixture of compounds **3** and **4** (4 : 1) was 13.3 g (57%), bp 116–121 °C (0.2 Torr). ^{31}P - $\{^1\text{H}\}$ spectrum, CDCl_3 : δ_{P} 129.8 ppm (s) (**3**) (80%), δ_{P} 130.0 ppm (s) (**4**) (20%).

Method B. In a 100 ml three-necked flask equipped with a stirrer, a reflux condenser, and an inlet for argon, were placed toluene (100 ml), 3-tert-butylacetylacetone **1** (11.2 g, 72 mmol), triethylamine (12.2 ml, 87 mmol), catalytic quantity of zinc chloride (250 mg) and 2-chloro-1,3,2-benzodioxaphosphole **2** (12.5 g, 72 mmol). The mixture was heated at 110 °C for 22 h and cooled. The precipitate was filtered off, the filtrate was concentrated on a rotary evaporator, the residue was diluted with pentane (50 ml) and kept at 4 °C in a refrigerator for 12 hours. The resulting precipitate was filtered off, the filtrate was concentrated on a rotary evaporator, and the residue was distilled in vacuum. Yield of compound **3** was 18.5 g (88%), bp 117–120 °C (0.1 Torr). IR (film), cm^{-1} : 3069, 2958, 2909, 2870, 1718, 1637, 1591, 1477, 1420, 1397, 1366, 1355, 1333, 1304, 1229, 1151, 1094, 1035, 1010, 978, 922, 845, 795, 744, 714, 666. ^1H NMR spectrum, δ ppm, J Hz: 7.11 and 6.99 two m (C_6H_4 , 4H), 4.84 ddd (H-5, 1H, $^2J_{\text{HH}}$ 2.3 Hz, $^4J_{\text{PH}}$ 1.1-1.2 Hz, $^4J_{\text{HH}}$ 1.1 Hz), 4.56 d (H-5, 1H, $^2J_{\text{HH}}$ 2.3 Hz), 3.01 d (H-3, 1H, $^4J_{\text{HH}}$ 1.1 Hz), 2.11 s (H-1, 3H), 0.99 s [$(\text{CH}_3)_3\text{C}$, 9H]. ^{13}C NMR spectrum, δ_{C} ppm, J Hz (hereinafter a view of signal in ^{13}C - $\{^1\text{H}\}$ NMR spectrum is in parentheses): 205.64 dq (s) (C^2 , $^2J_{\text{HC}^1\text{C}}$ 5.8 Hz, $^2J_{\text{HC}^3\text{C}}$ 5.8 Hz), 151.62 dtd (d) (C^4 , $^2J_{\text{HC}^3\text{C}}$ 7.1 Hz, $^2J_{\text{HC}^5\text{C}}$ 5.1 Hz, $^2J_{\text{POC}}$ 3.0 Hz), 144.70 dddd (d) (C^i , $^3J_{\text{HC}^m\text{CC}}$ 7.8-7.9 Hz, $^3J_{\text{HC}^o\text{CC}}$ 7.8-7.9 Hz, $^3J_{\text{POCC}}$ 7.9 Hz, $^2J_{\text{HC}^o\text{C}}$ 2.4 Hz), 122.96 ddd (d) (C^m , $^1J_{\text{HC}}$ 162.9 Hz, $^3J_{\text{HC}^o\text{CC}}$ 8.1 Hz, $^4J_{\text{POCCC}}$ 4.5 Hz), 112.8 br. ddd (br. d) (C^o , $^1J_{\text{HC}}$ 163.3 Hz, $^3J_{\text{HC}^m\text{CC}}$ 8.2 Hz, $^3J_{\text{POCC}}$ 4.1 Hz), 100.96 tdd (d) (C^5 , $^1J_{\text{HC}}$ 159.0 Hz, $^3J_{\text{POCC}}$ 15.1 Hz, $^3J_{\text{HC}^3\text{CC}}$ 3.3 Hz), 66.71 br. d (s) (C^3 , $^1J_{\text{HC}}$ 126.1 Hz), 34.08 ddecet (s) (Me_3C , $^2J_{\text{HC}^3\text{C}}$ 3.9 Hz, $^2J_{\text{HCC}}$ 3.9 Hz), 31.95 q (s) (C^1 , $^1J_{\text{HC}}$ 127.5 Hz), 28.23 qseptd (s) [$(\text{CH}_3)_3\text{C}$, $^1J_{\text{HC}}$ 125.6 Hz, $^3J_{\text{HCCC}}$ 4.5 Hz, $^3J_{\text{HCCC}}$ 4.2-4.4 Hz]. ^{31}P -

{¹H} NMR spectrum, 162.0 MHz, CDCl₃: δ_P 129.8 ppm (s). Mass-spectrum (ESI HRMS), *m/z*: 294.1022 [M]⁺ (Calculated 294.1021). Found, %: C, 61.11; H, 6.77; P, 10.44. Calculated for C₁₅H₁₉O₄P, %: C, 61.22; H, 6.51; P, 10.53.



3,3,7,7-Tetrakis(trifluoromethyl)-1,1-*o*-phenylenedioxa-5-(1-*tert*-butyl-2-oxopropyl)-2,6,8-trioxo-1-phosphabicyclo[4.3.2¹⁻⁵]octane 5. Hexafluoroacetone (4.65 g, 28 mmol) was condensed into a solution of compound **3** (4.0 g, 14 mmol) in CCl₄ (20 ml) cooled under argon to −40 °C. The mixture was kept until reaching 20 °C for 8 hours. The next day, a crystalline precipitate of compound **5** was formed, which was filtered and dried under vacuum (0.1 Torr). Yield was 5.7 g (67%), mp 107–109 °C. IR spectrum (Nujol), cm^{−1}: 1713, 1629, 1600, 1489, 1422, 1402, 1356, 1340, 1326, 1296, 1281, 1242, 1200, 1154, 1123, 1054, 1042, 1019, 974, 946, 925, 898, 878, 853, 839, 810, 775, 751, 723, 709, 700, 668, 636, 559, 547, 523, 504, 426. ¹H NMR spectrum, δ ppm, *J* Hz: 1.18 s [C(CH₃)₃, 9H], 2.24 s (H-18, 3H), 2.73 (C⁴H_x, 1H, ²*J*_{AX} 17.1 Hz, ⁴*J*_{FH} 1.0, ⁴*J*_{PH} 1.0), 3.49 s (H-16, 1H), 3.51 br. d (C⁴H_A, 1H, ²*J*_{AX} 17.1 Hz), 7.02 dddd (H-11, 1H, ³*J*_{H¹²H} 7.9 Hz, ⁴*J*_{H¹⁰H} 6.7 Hz, ⁵*J*_{PH} 2.4 Hz, ⁴*J*_{H⁹H} 1.3 Hz), 7.08-7.11 m, (H-9, H-10, 2H), 7.20 ddd (H-12, 1H, ³*J*_{H¹¹H} 7.9 Hz, ⁴*J*_{PH} 1.5-1.6 Hz, ³*J*_{H¹⁰H} 1.3-1.4 Hz). ¹³C NMR spectrum, δ_C ppm, *J* Hz: 209.44 m (s) (C¹⁷, ²*J*_{HC¹⁸C} 5.0-5.1, ²*J*_{HC¹⁶C} 2.9-3.1 Hz), 144.71 m (s) (C¹³, ³*J*_{HC¹¹CC} 8.2 Hz, ³*J*_{HC⁹CC} 6.8 Hz, ²*J*_{HC¹²C} 1.4-1.5 Hz), 140.53 dddd (d) (C⁸, ³*J*_{HC¹⁰CC} 12.0-12.5 Hz, ³*J*_{HC¹²CC} 8.2-8.5 Hz, ²*J*_{HC¹⁹C} 4.7-5.1 Hz, ²*J*_{POC} 3.3 Hz), 124.60 dd (s) (C¹¹, ¹*J*_{HC} 163.0 Hz, ³*J*_{HC⁹CC} 7.1 Hz), 122.39 ddd (s) (C¹⁰, ¹*J*_{HC} 165.7 Hz, ³*J*_{HC¹²CC} 7.3 Hz, ²*J*_{HC⁹C} 1.8 Hz), 122.04 qdq (qdq) (C²³F₃, ¹*J*_{FC} 290.1 Hz, ²*J*_{PC⁷C} 6.4 Hz, ³*J*_{FC²⁴C⁷C} 2.2 Hz), 121.74 qdd (q) (C¹⁵F₃, ¹*J*_{FC} 288.1 Hz, ³*J*_{HC⁴C³C} 7.0 Hz, ³*J*_{HC⁴C³C} 4.7 Hz), 121.20 br. qd (br. qd) (C²²F₃, ¹*J*_{FC} 286.0 Hz, ²*J*_{PC⁷C} 2.0 Hz), 121.13 br. qd (br. qdd) (C¹⁴F₃, ¹*J*_{FC} 285.6 Hz, ³*J*_{POC³C} 15.3-16.0 Hz, ³*J*_{HC⁴C³C} 5.6 Hz), 111.85 ddd (d) (C¹², ¹*J*_{HC} 167.1 Hz, ³*J*_{POC¹³C} 18.5 Hz, ³*J*_{HC¹⁰CC} 7.1 Hz), 111.46 ddddd (d) (C⁹, ¹*J*_{HC} 166.6 Hz, ³*J*_{POC⁸C} 12.6 Hz, ³*J*_{HC¹¹CC} 8.6 Hz, ²*J*_{HC¹⁰C} 1.2-1.3 Hz, ⁴*J*_{HC¹²CC¹⁰C} 1.2-1.3 Hz), 80.27 sept.d (sept.ddd) (C³, ²*J*_{FC^{14,15}C} 31.7 Hz, ²*J*_{POC} 7.8 Hz, ²*J*_{HC⁴C} 4.1 Hz, ²*J*_{HC⁴C} 1.7-1.8 Hz), 75.31 d.sept (d.sept) (C⁷, ¹*J*_{PC} 165.8 Hz, ²*J*_{FC^{23,24}C} 31.5 Hz), 103.87 br. dm (br. d) (C¹⁶, ¹*J*_{HC} 130.0 Hz, ³*J*_{POC⁵C} 1.8 Hz), 36.06 qd (s) (C¹⁸, ¹*J*_{HC} 127.9 Hz, ³*J*_{HC¹⁶CC} 1.0 Hz), 34.61 m (s) (C¹⁹, ²*J*_{HC²⁰⁻²²C} 3.9 Hz, ²*J*_{HC¹⁶C} 3.9 Hz), 33.96 br. td (br. s) (C⁴, ¹*J*_{HC} 135.6 Hz, ³*J*_{HC¹⁶CC} 4.4 Hz), 29.14 q.sept.d (s) (C²⁰⁻²², ¹*J*_{HC} 126.1 Hz, ³*J*_{HC²⁰⁻²²CC} 4.4 Hz, ³*J*_{HC¹⁶CC} 4.4 Hz). ¹⁹F NMR spectrum, δ_F ppm, *J* Hz: −67.94 m (C²³F₃, ⁴*J*_{FC²⁴CC²³F} 11.5-12.0 Hz, ⁷*J*_{FC¹⁵C²³F} 11.5-12.0 Hz), −68.01 m (C²⁴F₃, ⁴*J*_{FC²³CC²⁴F} 11.5 Hz, ³*J*_{PC⁷C²⁴F} 6.3 Hz), −73.63 q (C¹⁴F₃, ⁴*J*_{FC¹⁵CC¹⁴F} 11.5 Hz), −77.13 qq (C¹⁵F₃, ⁴*J*_{FC¹⁴CC¹⁵F} 11.5 Hz, ⁷*J*_{FC²³C¹⁵F} 11.5 Hz). ³¹P / ³¹P-¹H} NMR spectra, δ_P ppm, *J* Hz: −28.5

br. q (br. q) ($^3J_{\text{FCCP}}$ 5.0 Hz). Mass-spectrum (ESI HRMS), m/z : 626.0727 $[\text{M}]^{+\bullet}$ (Calculated 626.0728). Found, %: 40.11; H, 3.18; P, 5.03. Calculated for $\text{C}_{21}\text{H}_{19}\text{F}_{12}\text{O}_6\text{P}$, %: C, 40.27; H, 3.06; P, 4.95.

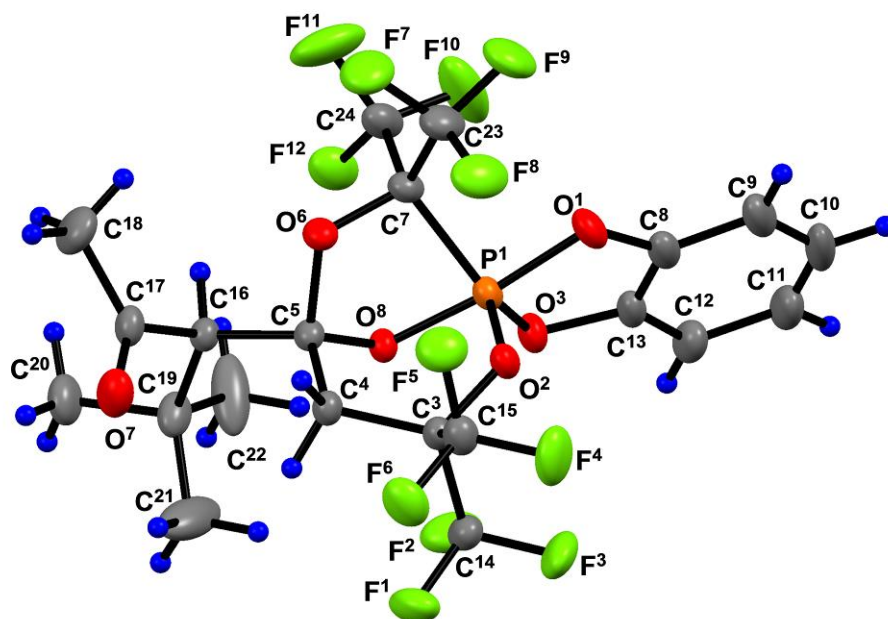


Figure S1. Geometry of molecule **5** in the crystal ($\text{P}^1_s\text{C}^5_s\text{C}^{16}_R / \text{P}^1_R\text{C}^5_R\text{C}^{16}_S$ -diastereoisomer, $\text{P}^1_R\text{C}^5_R\text{C}^{16}_S$ -enantiomer is shown). Non-hydrogen atoms are shown as thermal ellipsoids with a probability of 30%.

Table S1. Bond lengths in the molecule of compound (5).

bond	<i>d</i> , Å	bond	<i>d</i> , Å	bond	<i>d</i> , Å	bond	<i>d</i> , Å	bond	<i>d</i> , Å
P ¹ –O ¹	1.676(3)	F ⁴ –C ¹⁵	1.321(4)	O ¹ –C ⁸	1.381(4)	C ⁷ –C ²⁴	1.551(5)	C ¹⁷ –C ¹⁸	1.492(6)
P ¹ –O ²	1.603(3)	F ⁵ –C ¹⁵	1.316(4)	O ³ –C ¹³	1.394(4)	C ⁸ –C ⁹	1.381(5)	C ¹⁹ –C ²⁰	1.534(7)
P ¹ –O ³	1.618(3)	F ⁶ –C ¹⁵	1.329(4)	O ⁶ –C ⁷	1.409(4)	C ⁸ –C ¹³	1.361(5)	C ¹⁹ –C ²¹	1.501(8)
P ¹ –O ⁸	1.668(2)	F ⁷ –C ²³	1.330(5)	O ⁸ –C ⁵	1.397(4)	C ⁹ –C ¹⁰	1.411(8)	C ¹⁹ –C ²²	1.540(5)
P ¹ –C ⁷	1.899(4)	F ⁸ –C ²³	1.313(5)	C ³ –C ¹⁴	1.549(5)	C ¹⁰ –C ¹¹	1.370(9)	O ² –C ³	1.430(4)
F ¹ –C ¹⁴	1.311(4)	F ⁹ –C ²³	1.323(5)	C ⁴ –C ⁵	1.536(4)	C ¹¹ –C ¹²	1.395(6)	O ⁶ –C ⁵	1.488(4)
F ² –C ¹⁴	1.308(5)	F ¹⁰ –C ²⁴	1.316(5)	C ⁵ –C ¹⁶	1.553(4)	C ³ –C ⁴	1.551(4)	O ⁷ –C ¹⁷	1.202(5)
F ³ –C ¹⁴	1.327(4)	F ¹¹ –C ²⁴	1.312(6)	C ⁷ –C ²³	1.550(6)	C ¹⁶ –C ¹⁹	1.558(5)	C ³ –C ¹⁵	1.548(5)

Table S2. Bond angles in the molecule of compound (5).

Angle	φ (grad)	Angle	φ (grad)	Angle	φ (grad)	Angle	φ (grad)
O ¹ –P ¹ –O ²	91.5(1)	C ⁴ –C ³ –C ¹⁵	108.9(2)	F ¹⁰ –C ²⁴ –C ⁷	110.9(3)	F ¹ –C ¹⁴ –C ³	111.6(3)
O ¹ –P ¹ –O ³	91.7(1)	C ¹⁴ –C ³ –C ¹⁵	110.1(3)	F ¹¹ –C ²⁴ –C ⁷	112.5(4)	F ² –C ¹⁴ –F ³	106.9(3)
O ¹ –P ¹ –O ⁸	171.2(1)	C ³ –C ⁴ –C ⁵	113.3(2)	P ¹ –C ⁷ –O ⁶	103.4(2)	F ² –C ¹⁴ –C ³	111.8(3)
O ¹ –P ¹ –C ⁷	91.7(1)	O ⁶ –C ⁵ –O ⁸	106.0(2)	P ¹ –C ⁷ –C ²³	117.1(2)	F ³ –C ¹⁴ –C ³	111.9(3)
O ² –P ¹ –O ³	116.6(1)	O ⁶ –C ⁵ –C ⁴	107.7(2)	P ¹ –C ⁷ –C ²⁴	110.2(3)	F ⁴ –C ¹⁵ –F ⁵	107.1(3)
O ² –P ¹ –O ⁸	97.3(1)	O ⁶ –C ⁵ –C ¹⁶	103.9(2)	O ⁶ –C ⁷ –C ²³	105.2(3)	F ⁴ –C ¹⁵ –F ⁶	107.7(3)
O ² –P ¹ –C ⁷	107.5(1)	O ⁸ –C ⁵ –C ⁴	109.1(2)	O ⁶ –C ⁷ –C ²⁴	111.0(3)	F ⁴ –C ¹⁵ –C ³	112.8(3)
O ³ –P ¹ –O ⁸	85.2(1)	O ⁸ –C ⁵ –C ¹⁶	112.6(2)	C ²³ –C ⁷ –C ²⁴	109.5(3)	F ⁵ –C ¹⁵ –F ⁶	107.6(3)
O ³ –P ¹ –C ⁷	135.6(1)	C ⁴ –C ⁵ –C ¹⁶	116.7(3)	O ¹ –C ⁸ –C ⁹	126.8(4)	F ⁵ –C ¹⁵ –C ³	110.7(3)
O ⁸ –P ¹ –C ⁷	84.8(1)	C ⁵ –C ¹⁶ –C ¹⁷	107.7(2)	O ¹ –C ⁸ –C ¹³	111.3(3)	F ⁶ –C ¹⁵ –C ³	110.8(3)
P ¹ –O ¹ –C ⁸	111.7(2)	C ¹⁷ –C ¹⁶ –C ¹⁹	112.2(3)	C ⁹ –C ⁸ –C ¹³	121.8(4)	C ⁵ –C ¹⁶ –C ¹⁹	120.4(2)
P ¹ –O ² –C ³	125.7(2)	O ⁷ –C ¹⁷ –C ¹⁸	121.5(4)	C ⁸ –C ⁹ –C ¹⁰	115.2(4)	O ⁷ –C ¹⁷ –C ¹⁶	121.2(3)
P ¹ –O ³ –C ¹³	113.3(2)	C ¹⁶ –C ¹⁹ –C ²⁰	108.2(4)	C ⁹ –C ¹⁰ –C ¹¹	122.4(4)	C ¹⁶ –C ¹⁷ –C ¹⁸	117.3(3)
C ⁵ –O ⁶ –C ⁷	112.2(2)	C ¹⁶ –C ¹⁹ –C ²²	108.0(3)	C ¹⁰ –C ¹¹ –C ¹²	121.7(5)	C ¹⁶ –C ¹⁹ –C ²¹	114.8(4)
P ¹ –O ⁸ –C ⁵	111.1(2)	C ²⁰ –C ¹⁹ –C ²²	105.8(3)	C ¹¹ –C ¹² –C ¹³	115.2(4)	C ²⁰ –C ¹⁹ –C ²¹	111.1(4)
O ² –C ³ –C ⁴	114.9(2)	F ⁷ –C ²³ –F ⁸	107.5(4)	O ³ –C ¹³ –C ⁸	111.1(3)	C ²¹ –C ¹⁹ –C ²²	108.5(4)
O ² –C ³ –C ¹⁴	107.4(2)	F ⁷ –C ²³ –C ⁷	109.9(3)	O ³ –C ¹³ –C ¹²	125.2(3)	F ⁷ –C ²³ –F ⁹	107.4(3)
O ² –C ³ –C ¹⁵	103.2(2)	F ⁸ –C ²³ –C ⁷	111.5(3)	C ⁸ –C ¹³ –C ¹²	123.7(3)	F ⁸ –C ²³ –F ⁹	108.0(3)
C ⁴ –C ³ –C ¹⁴	112.0(2)	F ¹⁰ –C ²⁴ –F ¹¹	109.1(3)	F ¹ –C ¹⁴ –F ²	108.2(3)	F ⁹ –C ²³ –C ⁷	112.4(3)

Table S3. Torsion angles in the molecule of compound (5).

Angle	τ (grad)	Angle	τ (grad)	Angle	τ (grad)	Angle	τ (grad)
O ² -P ¹ -O ¹ -C ⁸	107.7(2)	O ³ -P ¹ -C ⁷ -O ⁶	114.9(2)	C ⁴ -C ³ -C ¹⁵ -F ⁶	59.5(3)	C ²⁴ -C ⁷ -C ²³ -F ⁷	72.4(4)
O ³ -P ¹ -O ¹ -C ⁸	-9.0(2)	O ⁸ -P ¹ -C ⁷ -O ⁶	37.2(2)	C ¹⁴ -C ³ -C ¹⁵ -F ⁴	57.2(4)	C ²⁴ -C ⁷ -C ²³ -F ⁸	-168.6(3)
C ⁷ -P ¹ -O ¹ -C ⁸	-144.7(2)	P ¹ -O ¹ -C ⁸ -C ¹³	7.3(3)	C ¹⁴ -C ³ -C ¹⁵ -F ⁶	-63.6(3)	C ²⁴ -C ⁷ -C ²³ -F ⁹	-47.1(4)
O ¹ -P ¹ -O ² -C ³	173.0(2)	P ¹ -O ² -C ³ -C ¹⁴	92.2(3)	O ² -C ³ -C ¹⁴ -F ³	54.4(4)	P ¹ -C ⁷ -C ²⁴ -F ¹⁰	-56.2(4)
O ³ -P ¹ -O ² -C ³	-94.3(2)	P ¹ -O ² -C ³ -C ¹⁵	-151.5(2)	O ² -C ³ -C ¹⁵ -F ⁵	62.8(3)	P ¹ -C ⁷ -C ²⁴ -F ¹¹	-178.7(3)
O ⁸ -P ¹ -O ² -C ³	-6.1(2)	P ¹ -O ² -C ³ -C ⁴	-33.1(3)	C ¹⁵ -C ³ -C ¹⁴ -F ²	-177.2(3)	P ¹ -C ⁷ -C ²⁴ -F ¹²	62.3(4)
C ⁷ -P ¹ -O ² -C ³	80.7(2)	P ¹ -O ³ -C ¹³ -C ¹²	173.6(3)	C ⁴ -C ³ -C ¹⁴ -F ³	-178.7(3)	O ⁶ -C ⁷ -C ²⁴ -F ¹⁰	-170.1(3)
O ¹ -P ¹ -O ³ -C ¹³	8.3(2)	C ⁵ -O ⁶ -C ⁷ -C ²³	-145.8(2)	C ¹⁵ -C ³ -C ¹⁴ -F ¹	61.5(3)	O ⁶ -C ⁷ -C ²⁴ -F ¹¹	67.4(4)
O ² -P ¹ -O ³ -C ¹³	-84.2(2)	C ⁵ -O ⁶ -C ⁷ -P ¹	-22.4(3)	C ¹⁴ -C ³ -C ¹⁵ -F ⁵	177.1(3)	O ⁶ -C ⁷ -C ²⁴ -F ¹²	-51.7(4)
O ⁸ -P ¹ -O ³ -C ¹³	-179.9(2)	C ⁷ -O ⁶ -C ⁵ -C ⁴	109.6(3)	C ¹⁵ -C ³ -C ¹⁴ -F ³	-57.3(4)	C ²³ -C ⁷ -C ²⁴ -F ¹⁰	74.1(4)
C ⁷ -P ¹ -O ³ -C ¹³	102.6(2)	C ⁷ -O ⁶ -C ⁵ -C ¹⁶	-126.0(2)	O ² -C ³ -C ¹⁵ -F ⁴	-57.2(3)	C ²³ -C ⁷ -C ²⁴ -F ¹¹	-48.4(4)
O ² -P ¹ -O ⁸ -C ⁵	62.1(2)	C ⁷ -O ⁶ -C ⁵ -O ⁸	-7.1(3)	C ⁴ -C ³ -C ¹⁴ -F ¹	-59.9(4)	C ²³ -C ⁷ -C ²⁴ -F ¹²	-167.4(3)
O ³ -P ¹ -O ⁸ -C ⁵	178.4(2)	C ⁵ -O ⁶ -C ⁷ -C ²⁴	95.8(3)	C ⁴ -C ³ -C ¹⁴ -F ²	61.5(3)	O ⁶ -C ⁷ -C ²³ -F ⁷	-47.0(3)
C ⁷ -P ¹ -O ⁸ -C ⁵	-44.9(2)	P ¹ -O ⁸ -C ⁵ -C ¹⁶	152.4(2)	C ³ -C ⁴ -C ⁵ -C ¹⁶	157.9(3)	O ⁶ -C ⁷ -C ²³ -F ⁸	72.0(4)
O ⁸ -P ¹ -C ⁷ -C ²³	152.4(3)	P ¹ -O ⁸ -C ⁵ -O ⁶	39.4(2)	C ³ -C ⁴ -C ⁵ -O ⁶	-85.8(3)	P ¹ -C ⁷ -C ²³ -F ⁷	-161.2(2)
O ¹ -P ¹ -C ⁷ -C ²⁴	90.4(2)	P ¹ -O ⁸ -C ⁵ -C ⁴	-76.3(2)	C ³ -C ⁴ -C ⁵ -O ⁸	28.9(3)	P ¹ -C ⁷ -C ²³ -F ⁸	-42.2(4)
O ² -P ¹ -C ⁷ -C ²⁴	-177.5(2)	C ¹⁴ -C ³ -C ⁴ -C ⁵	-100.0(3)	O ⁶ -C ⁵ -C ¹⁶ -C ¹⁹	162.2(3)	C ⁵ -C ¹⁶ -C ¹⁷ -O ⁷	-71.1(4)
O ³ -P ¹ -C ⁷ -C ²⁴	-3.8(3)	O ² -C ³ -C ¹⁴ -F ²	-65.5(3)	C ⁴ -C ⁵ -C ¹⁶ -C ¹⁷	51.0(3)	C ⁵ -C ¹⁶ -C ¹⁷ -C ¹⁸	108.4(3)
O ⁸ -P ¹ -C ⁷ -C ²⁴	-81.5(2)	C ¹⁵ -C ³ -C ⁴ -C ⁵	138.0(3)	C ⁴ -C ⁵ -C ¹⁶ -C ¹⁹	-79.4(4)	C ¹⁹ -C ¹⁶ -C ¹⁷ -O ⁷	63.7(4)
O ¹ -P ¹ -C ⁷ -C ²³	-35.7(3)	O ² -C ³ -C ¹⁴ -F ¹	173.1(3)	O ⁶ -C ⁵ -C ¹⁶ -C ¹⁷	-67.4(3)	C ¹⁹ -C ¹⁶ -C ¹⁷ -C ¹⁸	-116.8(4)
O ² -P ¹ -C ⁷ -C ²³	56.4(3)	O ² -C ³ -C ⁴ -C ⁵	22.8(4)	O ⁸ -C ⁵ -C ¹⁶ -C ¹⁷	178.3(2)	C ⁵ -C ¹⁶ -C ¹⁹ -C ²⁰	-70.6(4)
O ³ -P ¹ -C ⁷ -C ²³	-129.9(3)	O ² -C ³ -C ¹⁵ -F ⁶	-178.0(2)	O ⁸ -C ⁵ -C ¹⁶ -C ¹⁹	47.9(4)	C ⁵ -C ¹⁶ -C ¹⁹ -C ²¹	54.1(5)
O ¹ -P ¹ -C ⁷ -O ⁶	-150.9(2)	C ⁴ -C ³ -C ¹⁵ -F ⁴	-179.7(3)	P ¹ -C ⁷ -C ²³ -F ⁹	79.3(3)	C ⁵ -C ¹⁶ -C ¹⁹ -C ²²	175.3(3)
O ² -P ¹ -C ⁷ -O ⁶	-58.8(2)	C ⁴ -C ³ -C ¹⁵ -F ⁵	-59.7(3)	O ⁶ -C ⁷ -C ²³ -F ⁹	-166.5(3)	C ¹⁷ -C ¹⁶ -C ¹⁹ -C ²¹	-74.3(4)

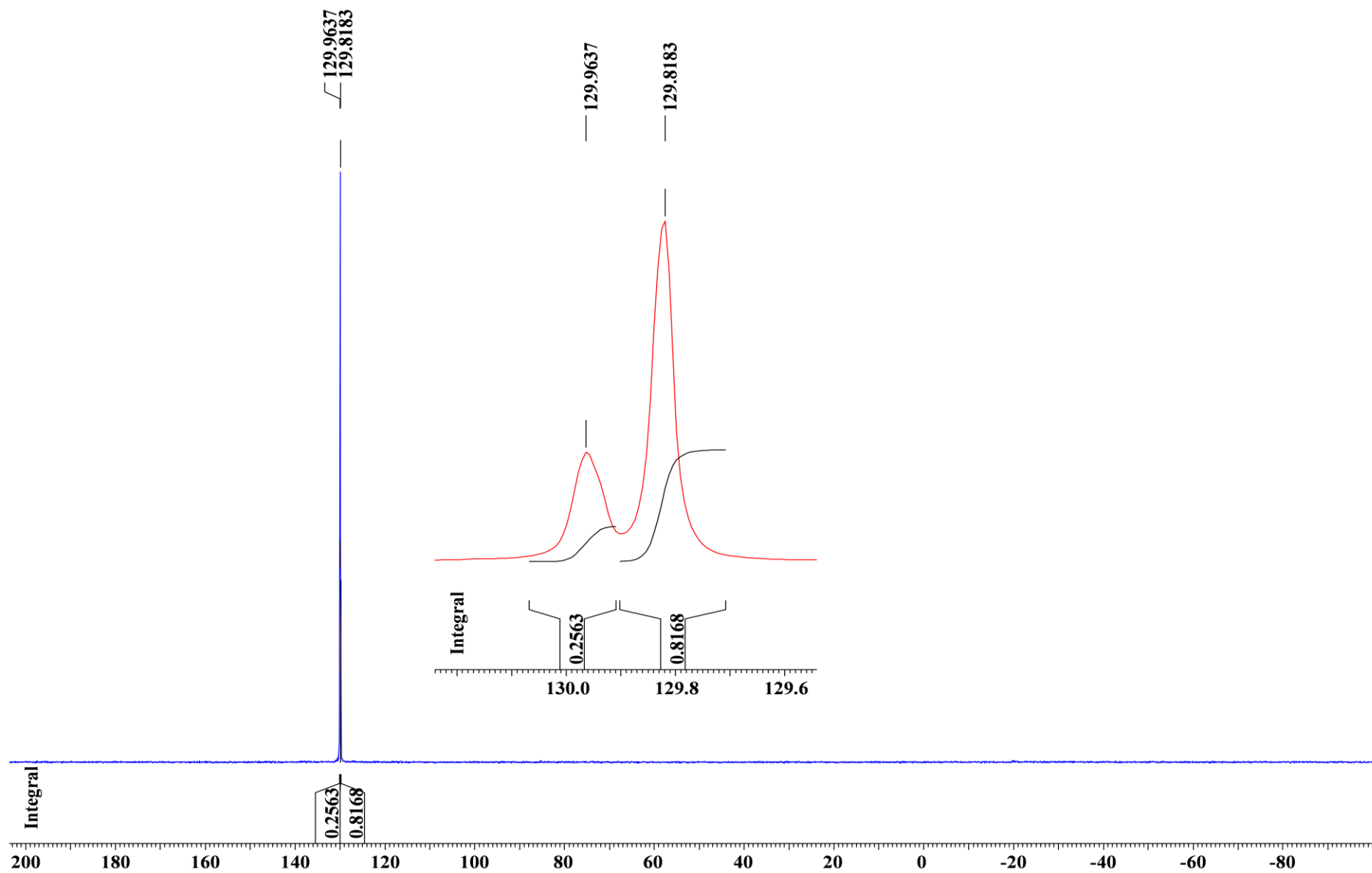


Figure S2. ^{31}P - $\{^1\text{H}\}$ NMR spectrum (162.0 MHz, CDCl_3 , 25°C) of phospholes (**3**, **4**) mixture (procedure *a*).

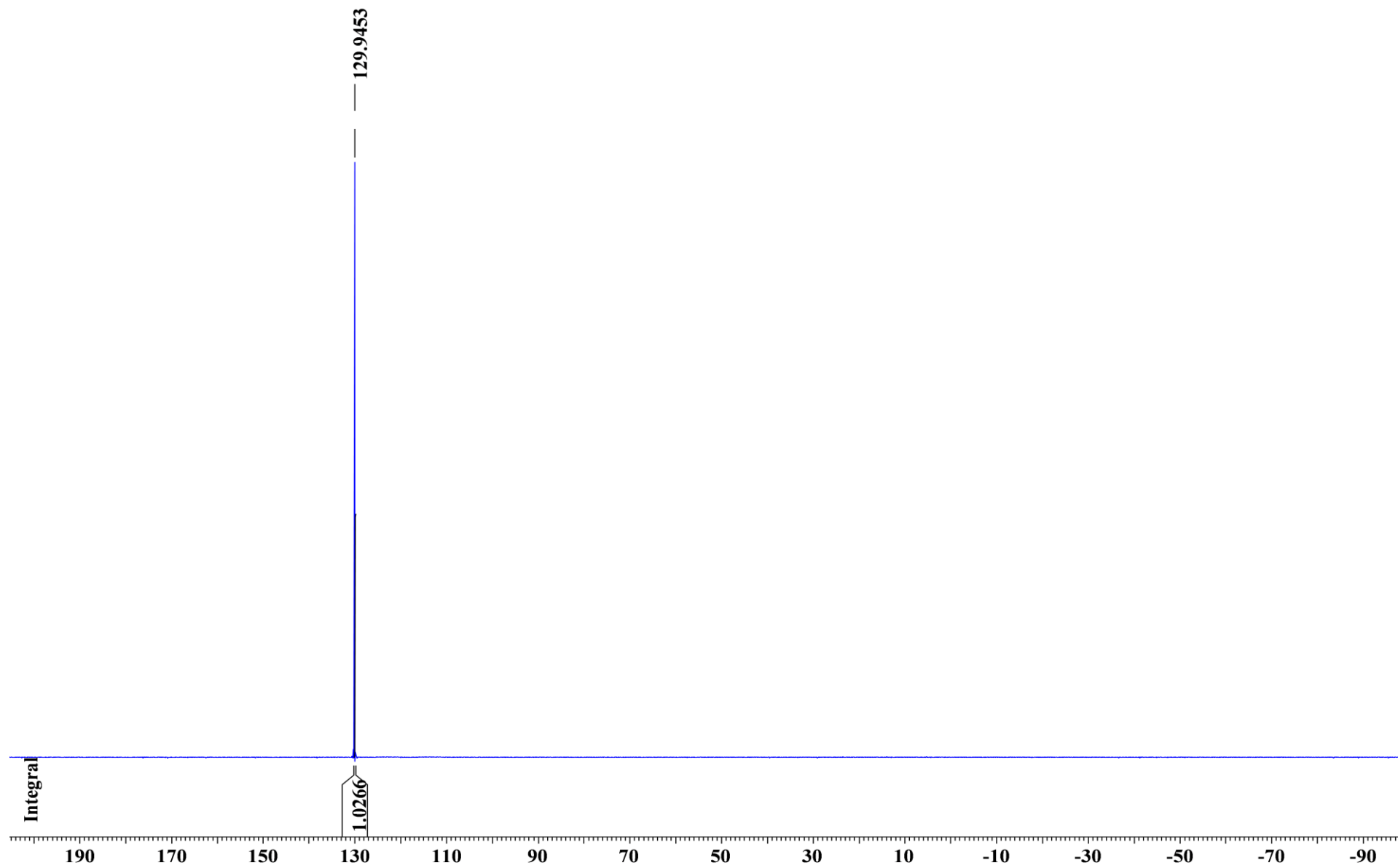


Figure S3. $^{31}\text{P}\{-^1\text{H}\}$ NMR spectrum (162.0 MHz, CDCl_3 , 25°C) of phosphole (**3**) (procedure *b*).

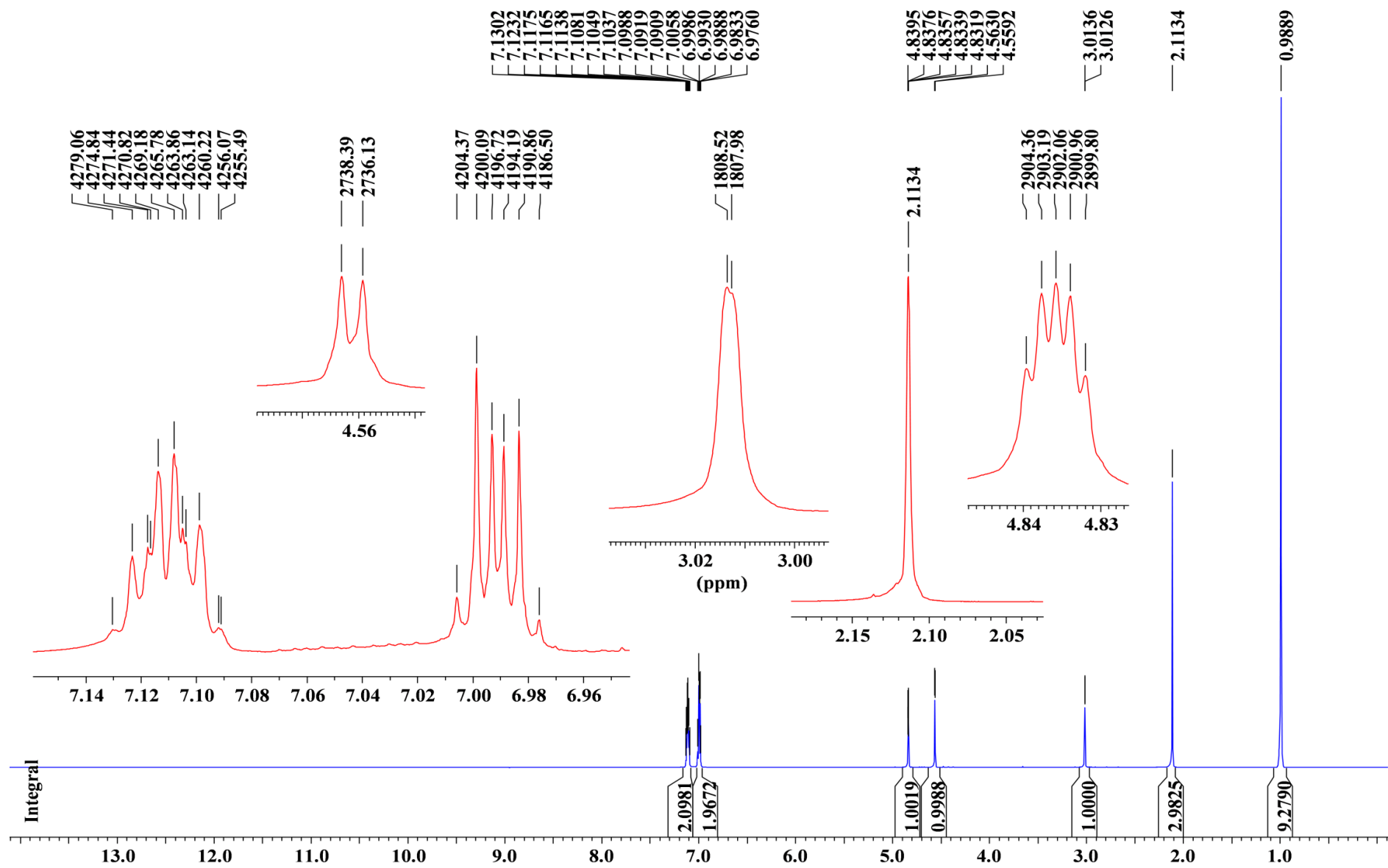


Figure S4. ¹H NMR spectrum (400.0 MHz, CDCl₃, 25°C) of phosphole (3).

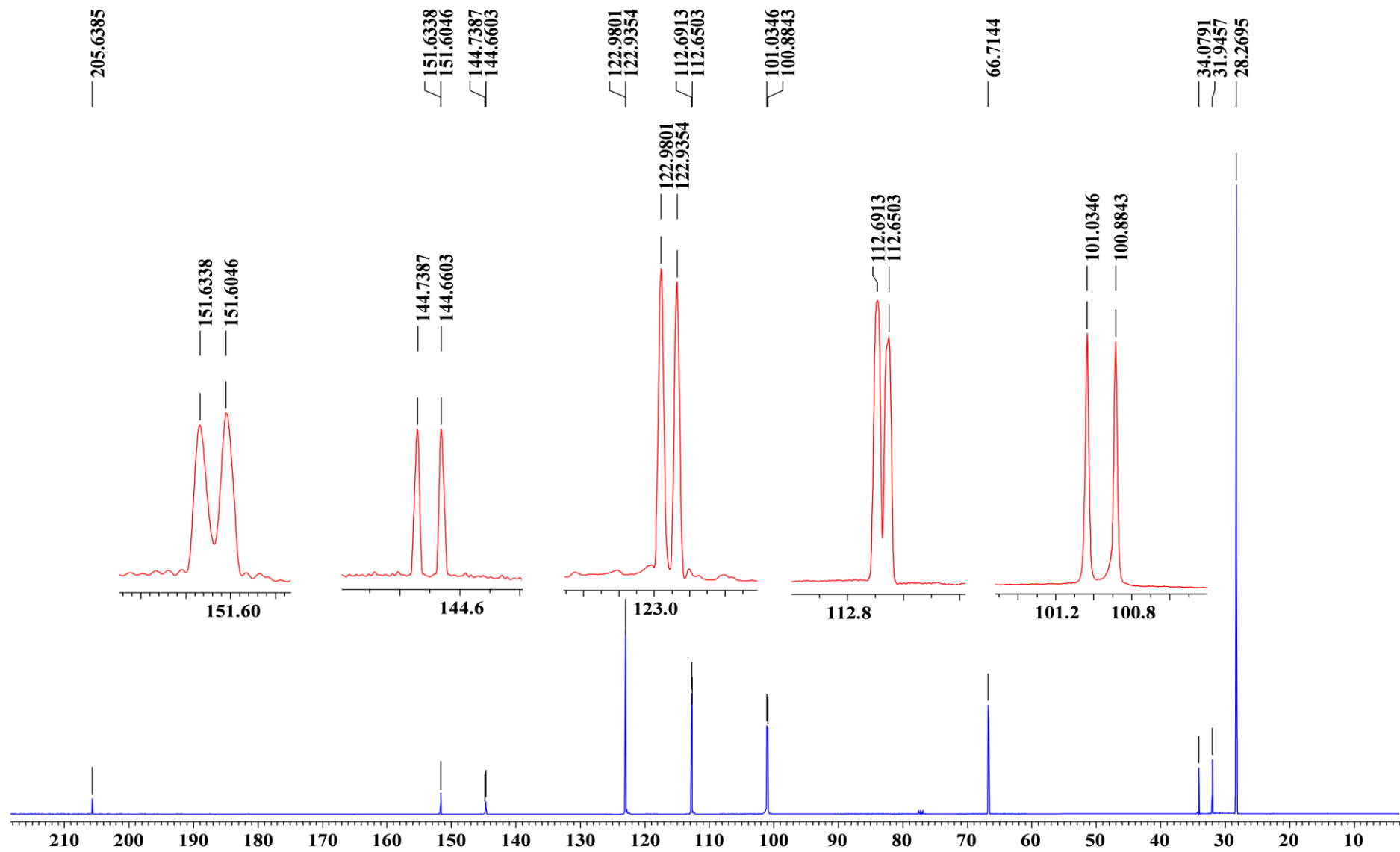


Figure S5. ^{13}C - $\{^1\text{H}\}$ NMR spectrum (100.6 MHz, CDCl_3 , 25°C) of phosphole (3).

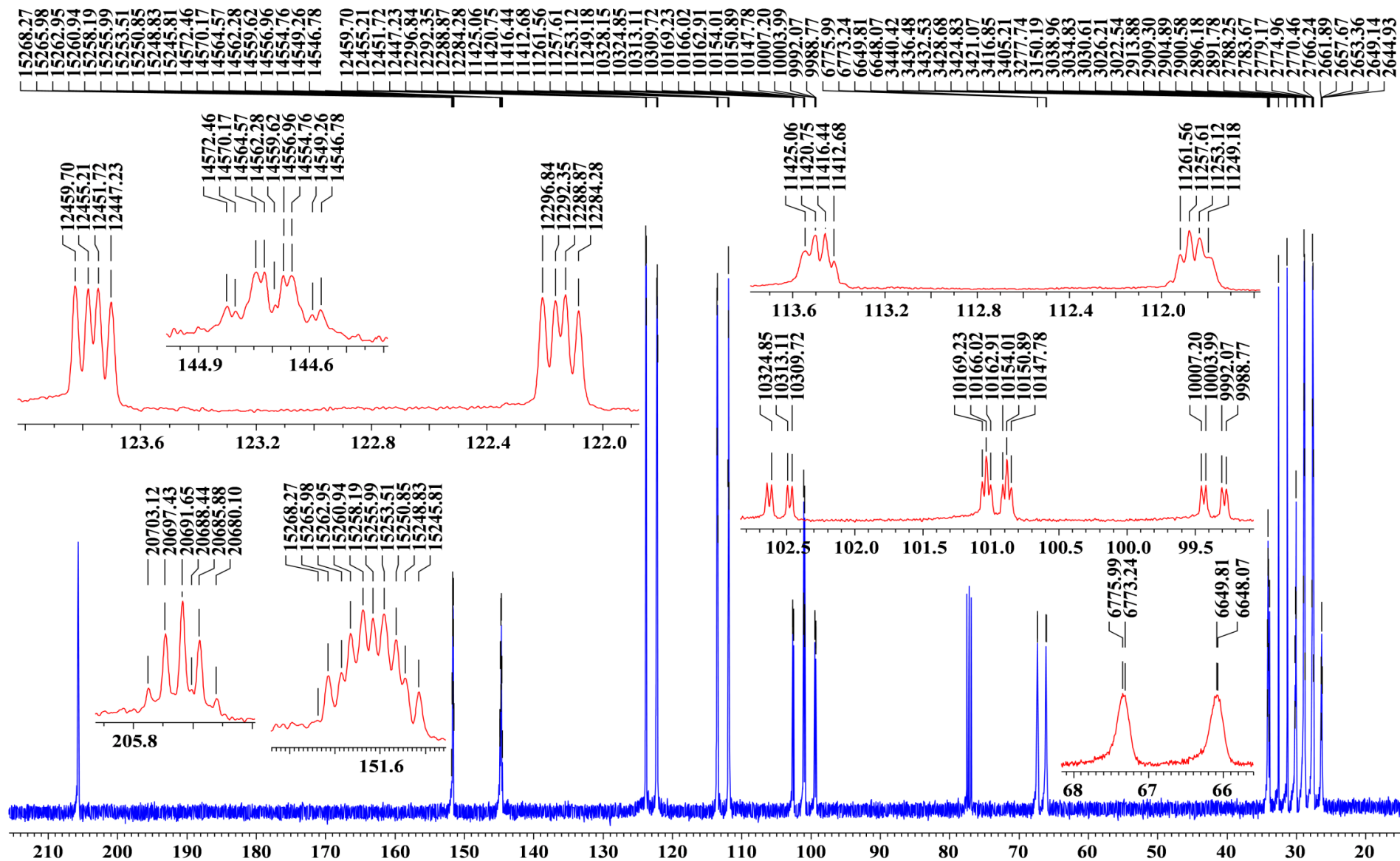


Figure S6. ^{13}C NMR spectrum (100.6 MHz, CDCl_3 , 25°C) of phosphole (3).

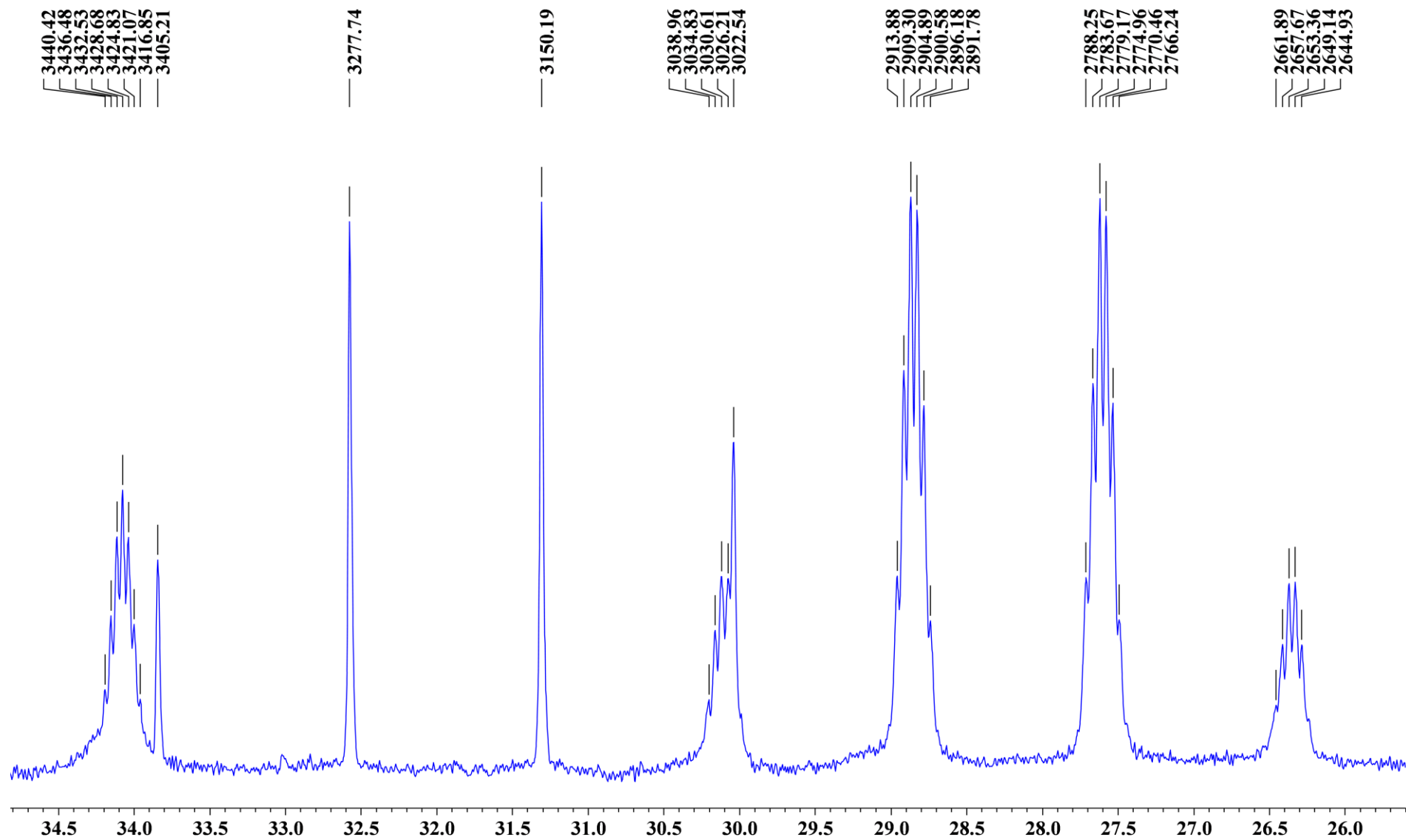


Figure S7. High-field region of ^{13}C NMR spectrum (100.6 MHz, CDCl_3 , 25°C) of phosphole (**3**).

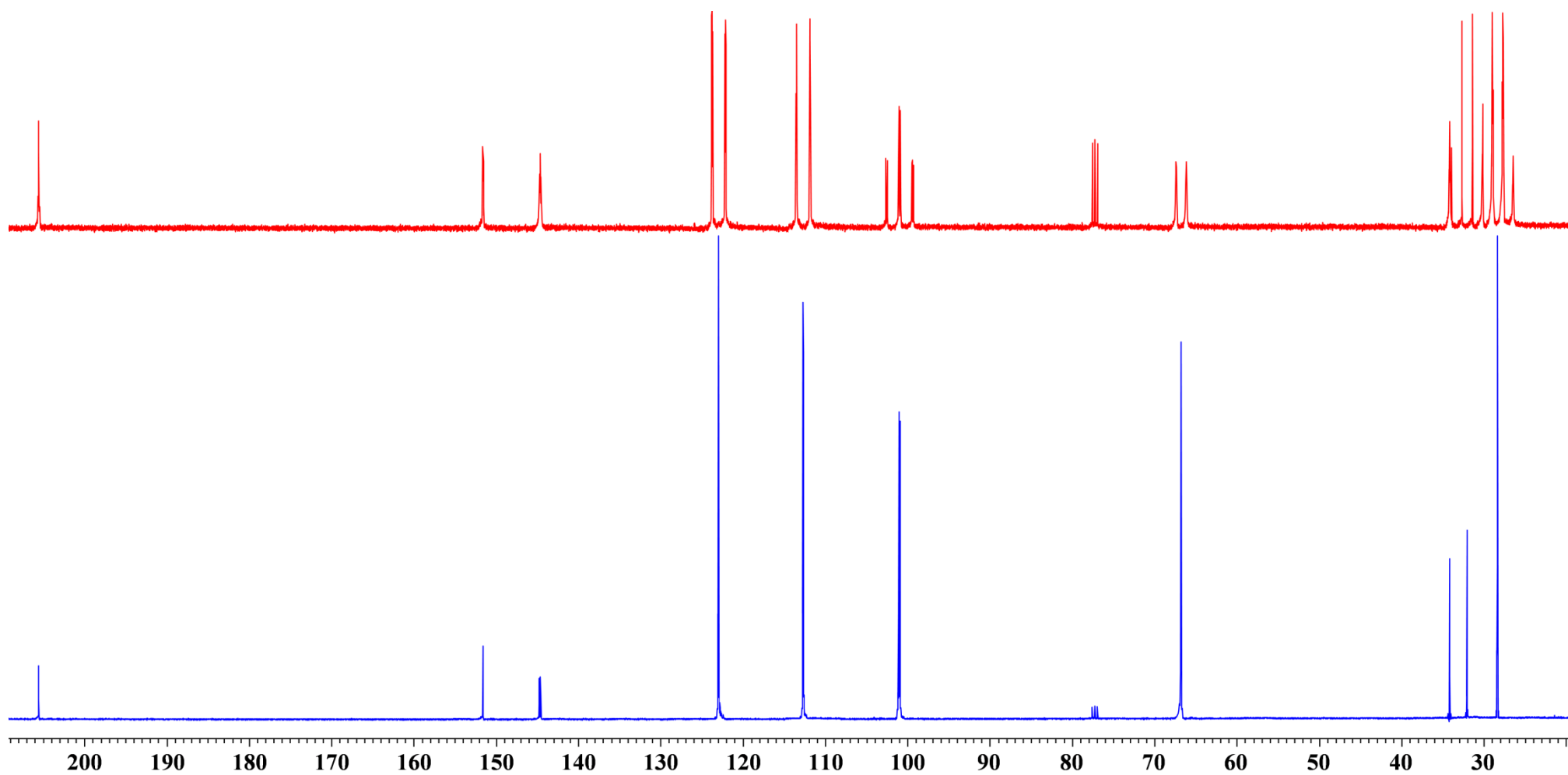


Figure S8. ^{13}C and $^{13}\text{C}\{-^1\text{H}\}$ NMR spectra (100.6 MHz, CDCl_3 , 25°C) of phosphole (**3**).

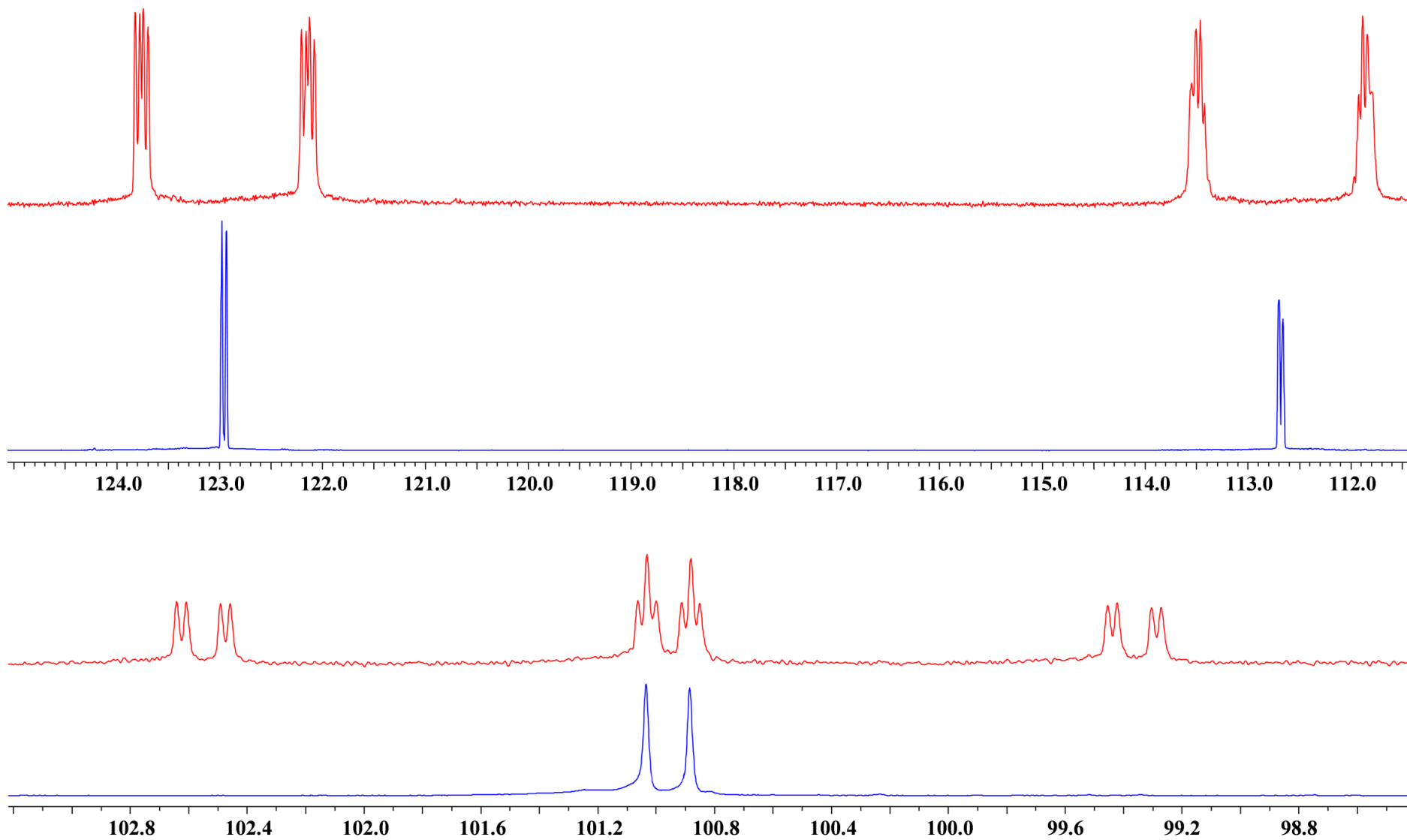


Figure S9. The fragments of ^{13}C and $^{13}\text{C}\{-^1\text{H}\}$ NMR spectra (100.6 MHz, CDCl_3 , 25°C) of phosphole (3).

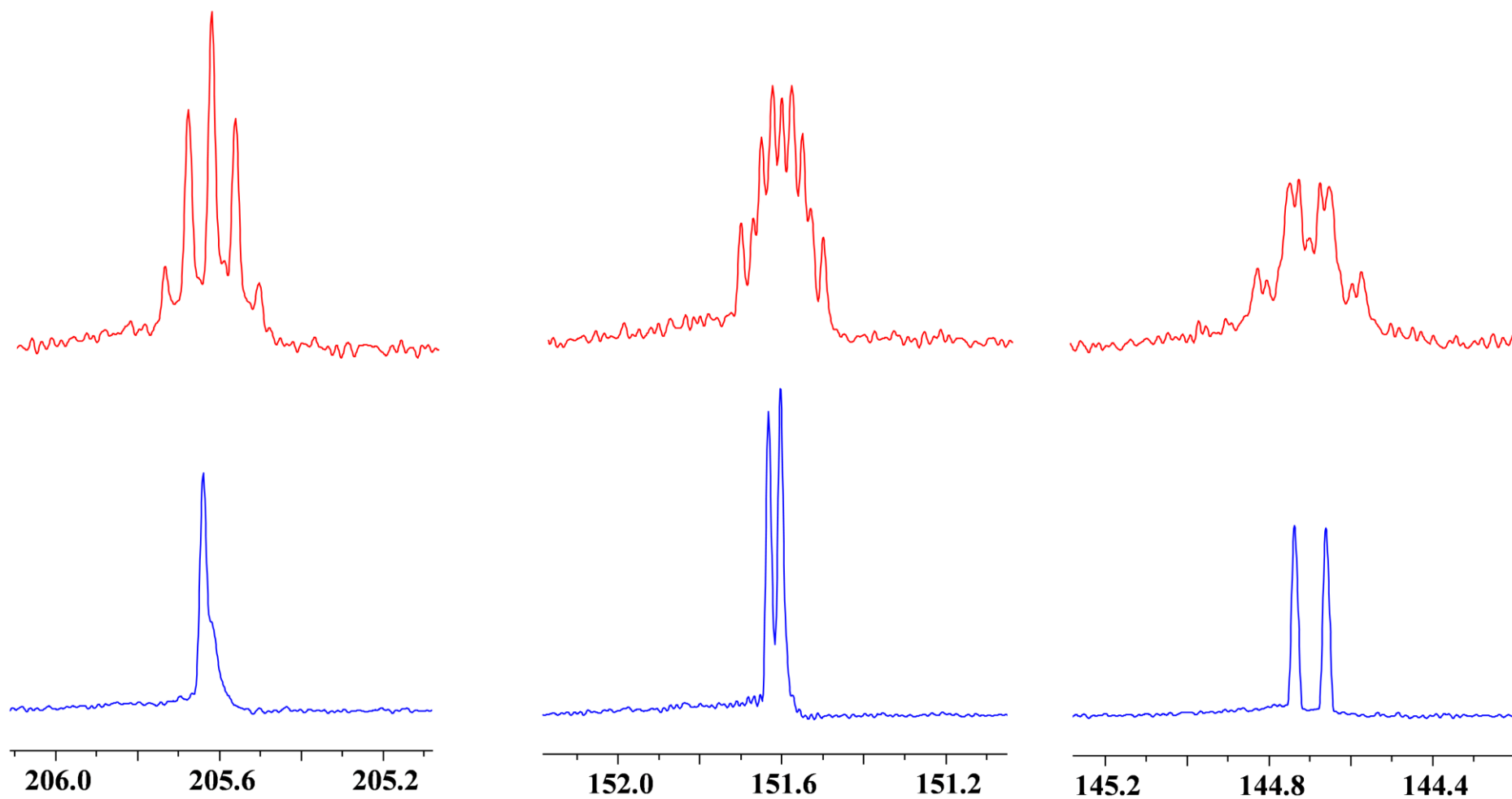


Figure S10. The low-field fragments of ^{13}C and $^{13}\text{C}\{-^1\text{H}\}$ NMR spectra (100.6 MHz, CDCl_3 , 25°C) of phosphole (**3**).

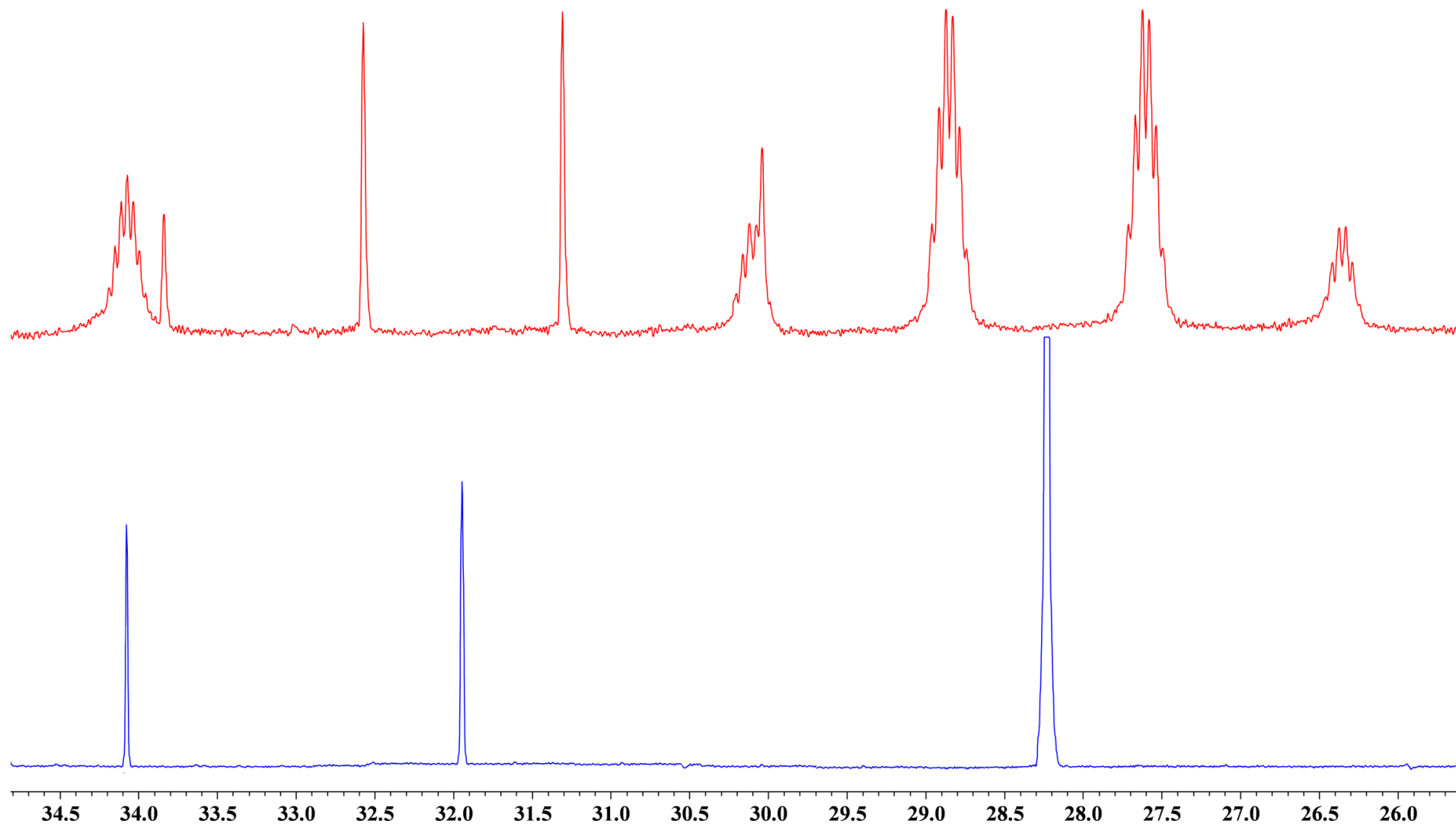


Figure S11. The high-field fragments of ^{13}C and $^{13}\text{C}\{-^1\text{H}\}$ NMR spectra (100.6 MHz, CDCl_3 , 25°C) of phosphole (**3**).

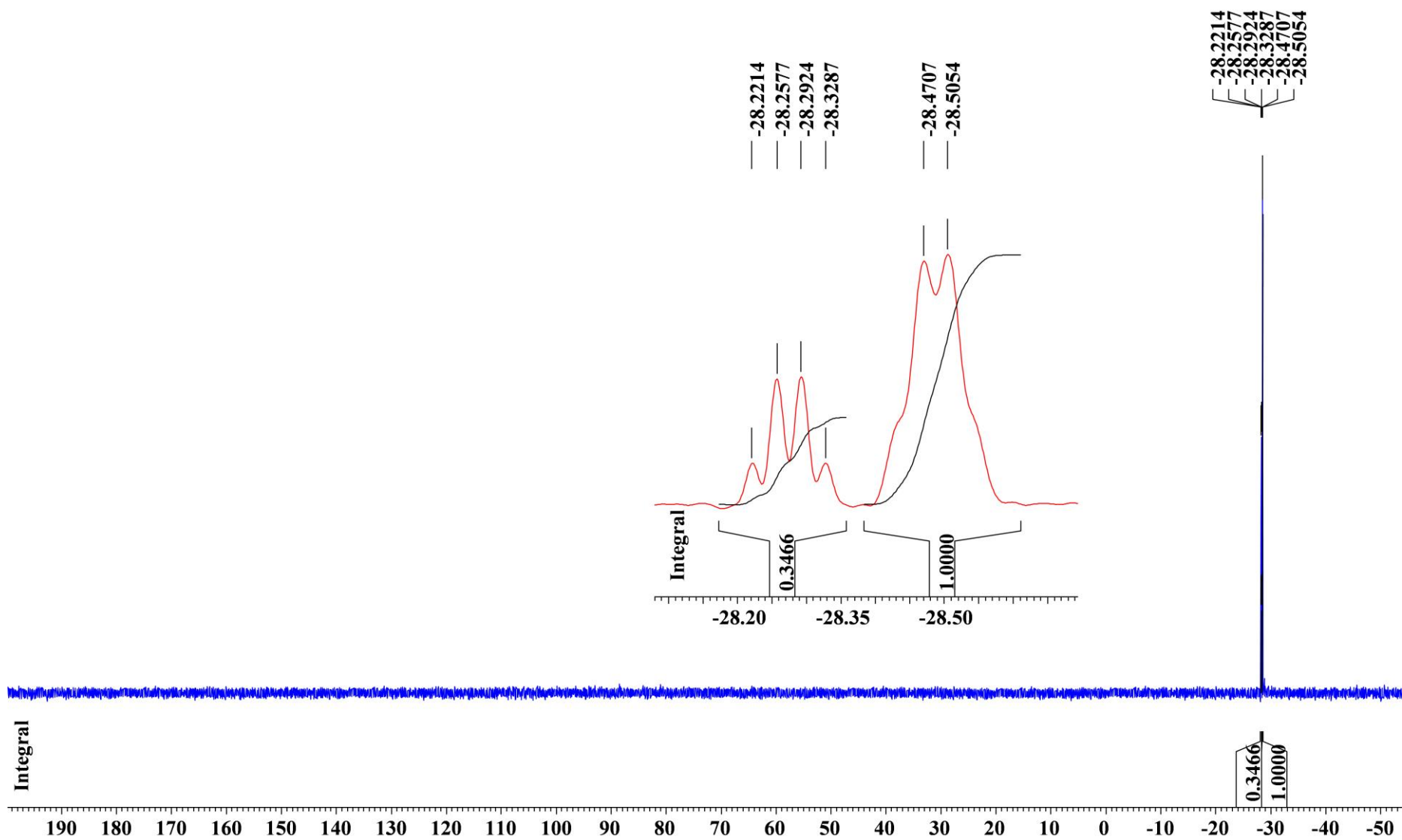


Figure S12. $^{31}\text{P}\{-^1\text{H}\}$ NMR spectrum (162.0 MHz, CDCl_3 , 25°C) of phosphoranes (**5**, **6**) mixture.

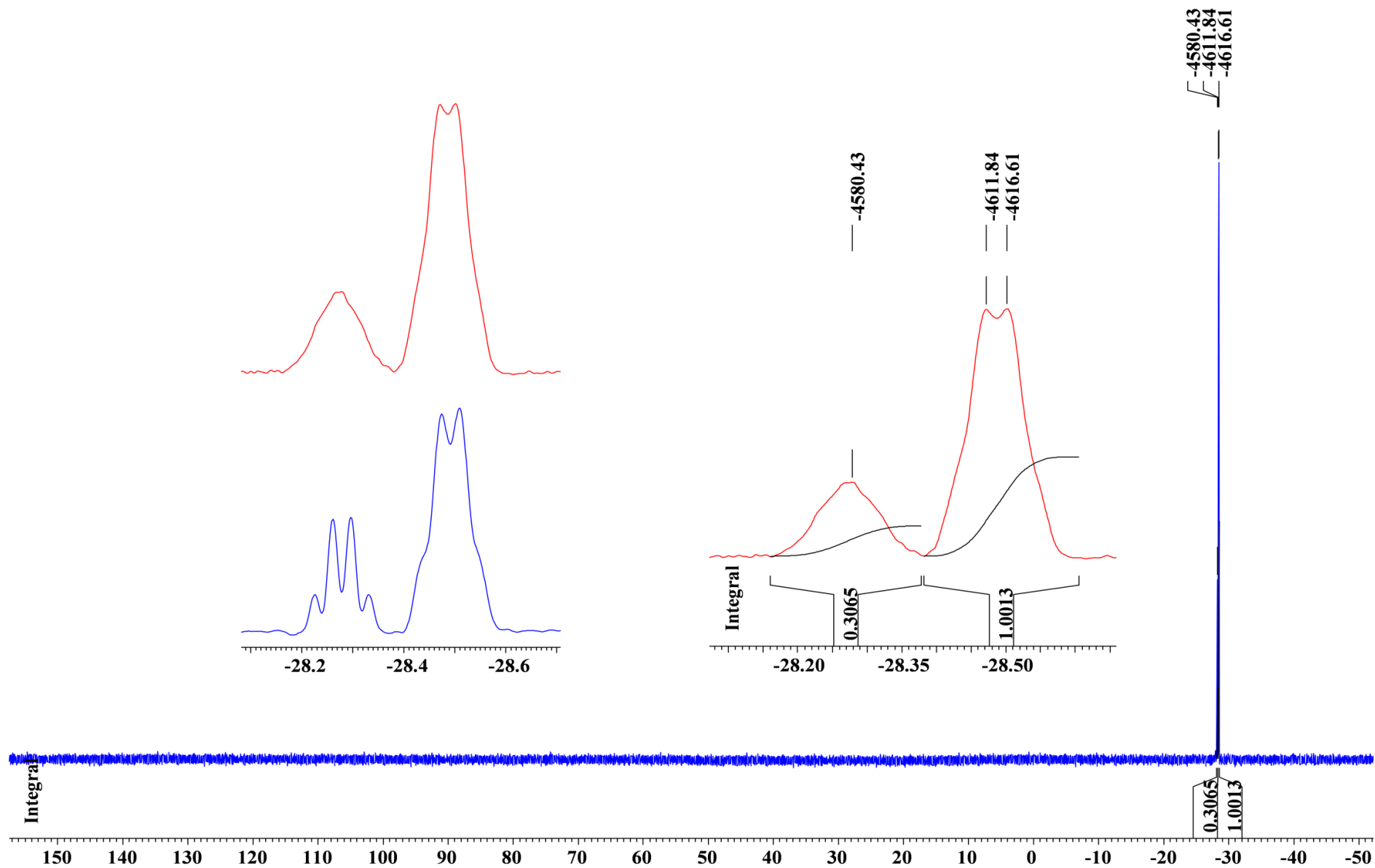


Figure S13. ^{31}P and $^{31}\text{P}\{-^1\text{H}\}$ NMR spectra (162.0 MHz, CDCl_3 , 25°C) of phosphoranes (5, 6) mixture.

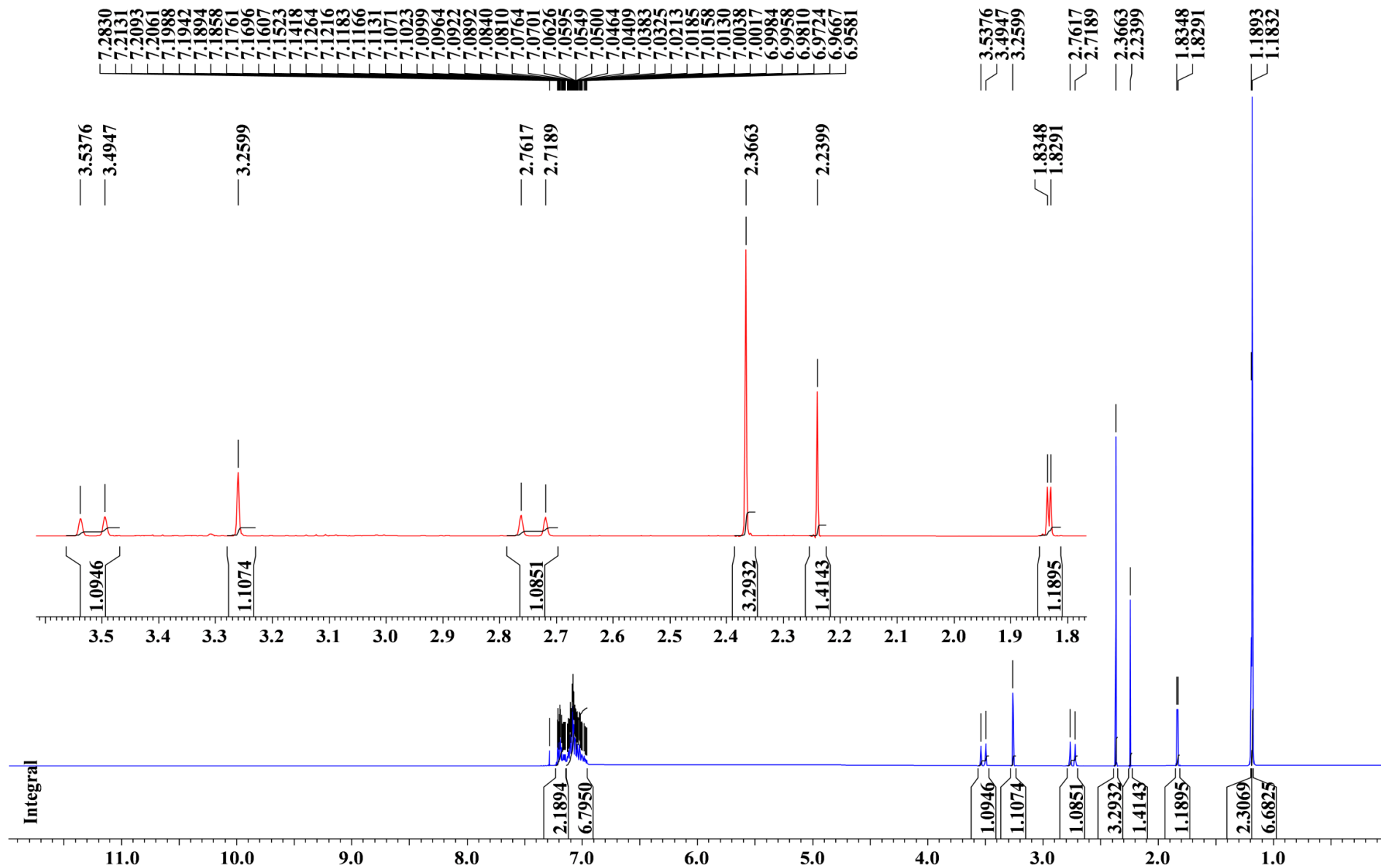


Figure S14. ^1H NMR spectrum (400.0 MHz, CDCl_3 , 25°C) of phosphoranes (**5**, **6**) mixture.

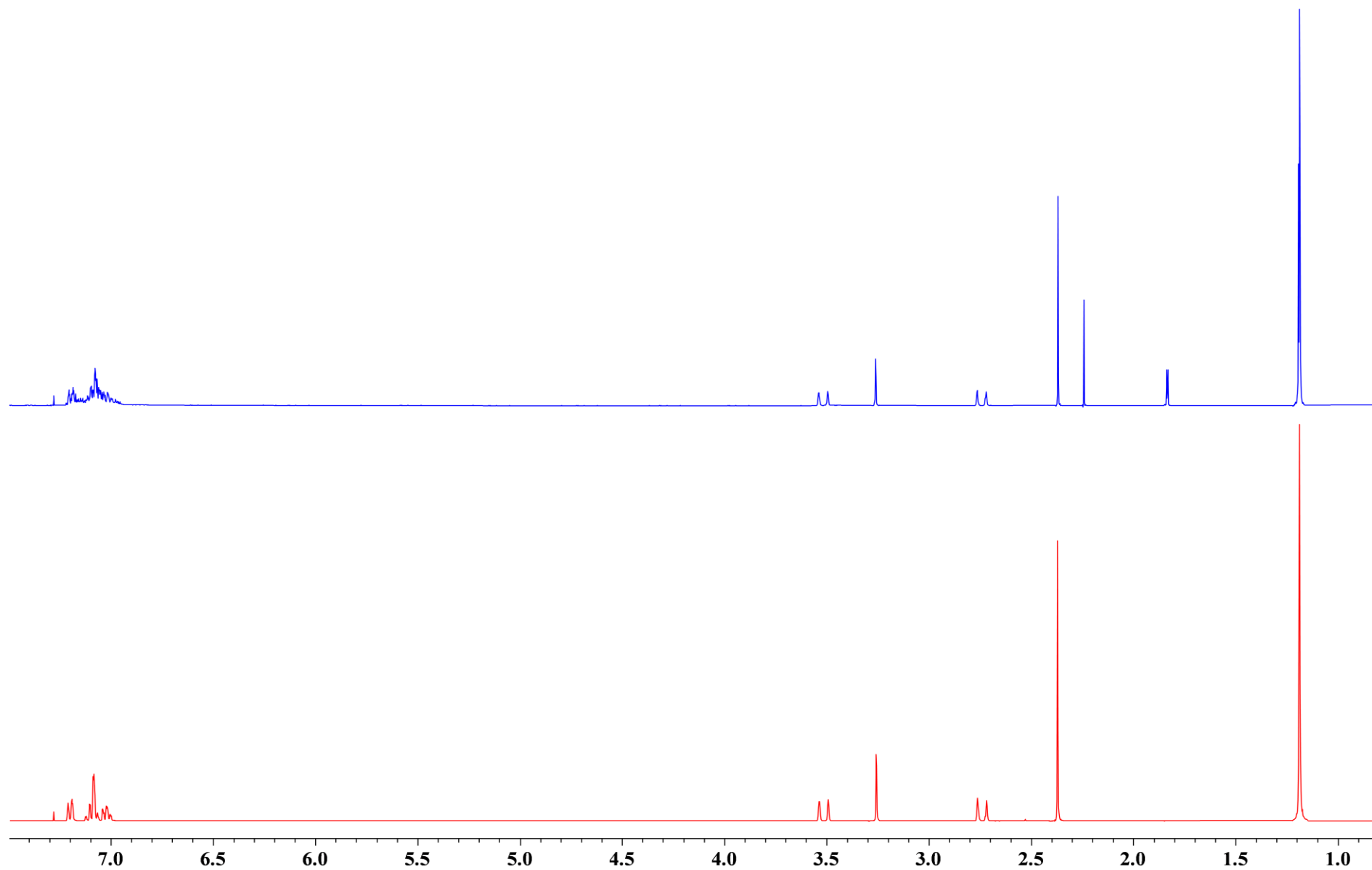


Figure S15. ^1H NMR spectra (400.0 MHz, CDCl_3 , 25°C) of phosphoranes (5, 6) mixture (blue) and phosphorane (6).

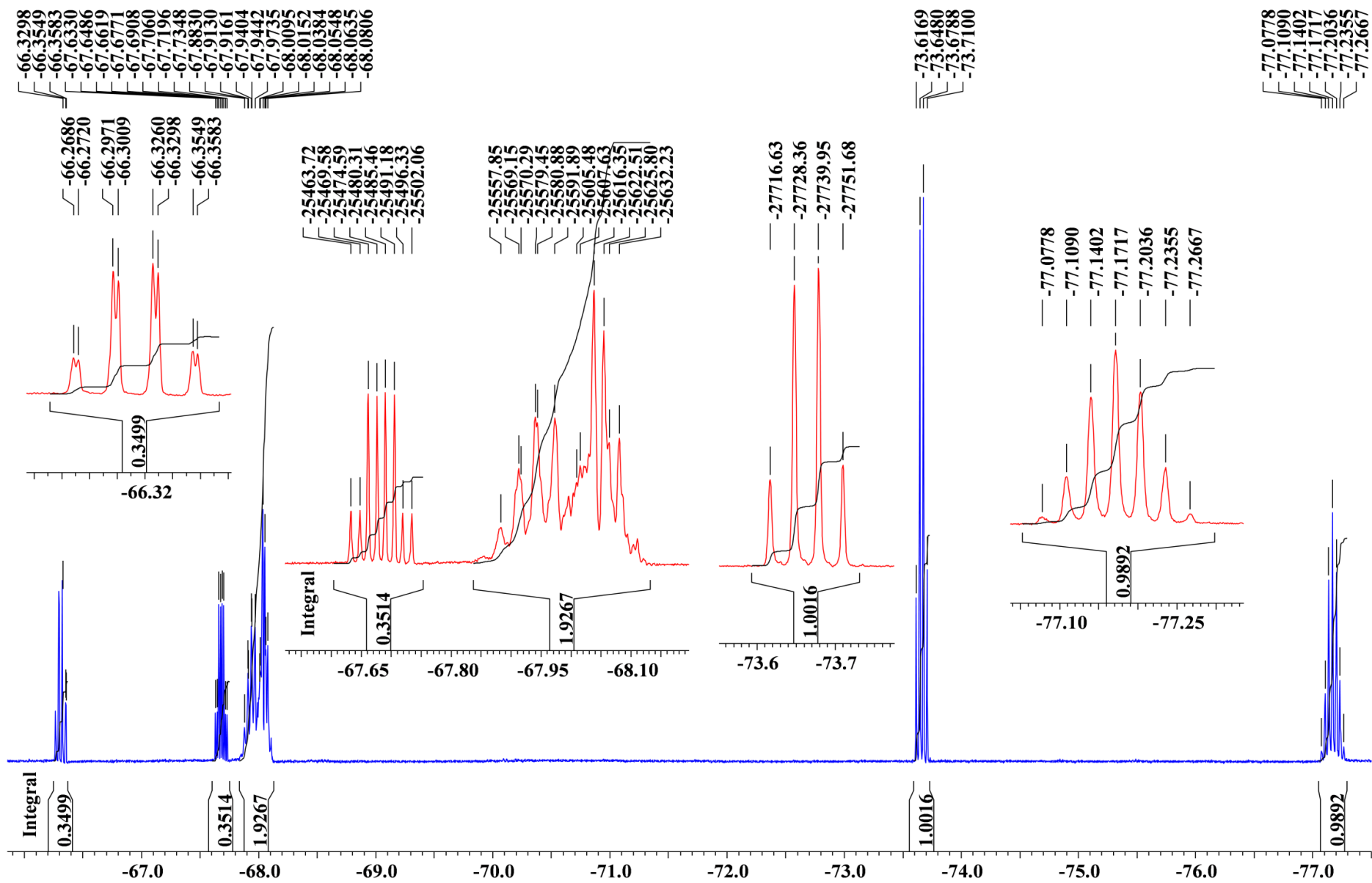


Figure S16. ^{19}F NMR spectrum (386.5 MHz, CDCl_3 , 25°C) of phosphoranes (**5**, **6**) mixture.

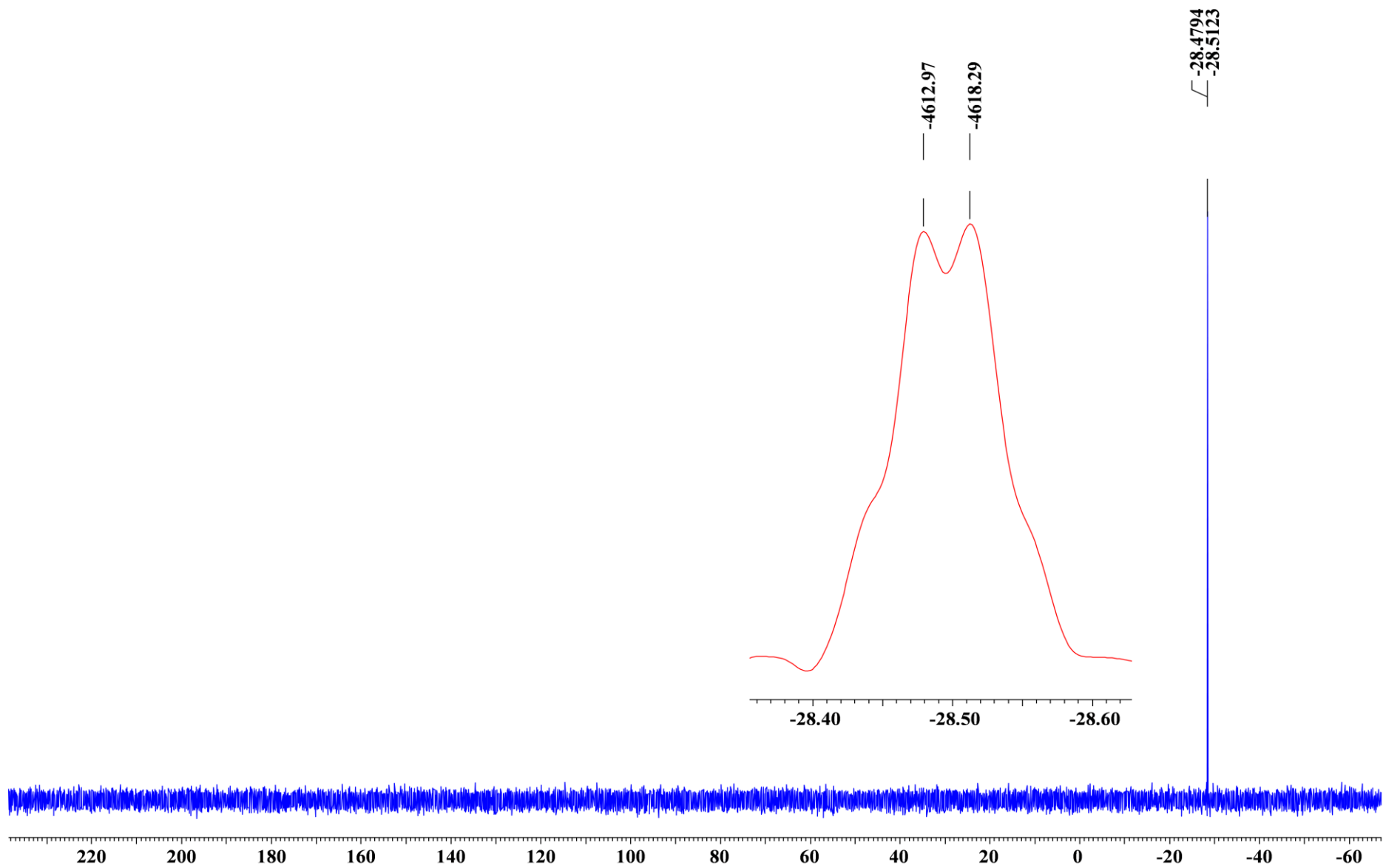


Figure S17. $^{31}\text{P}\{-^1\text{H}\}$ NMR spectrum (162.0 MHz, CDCl_3 , 25°C) of phosphorane (6).

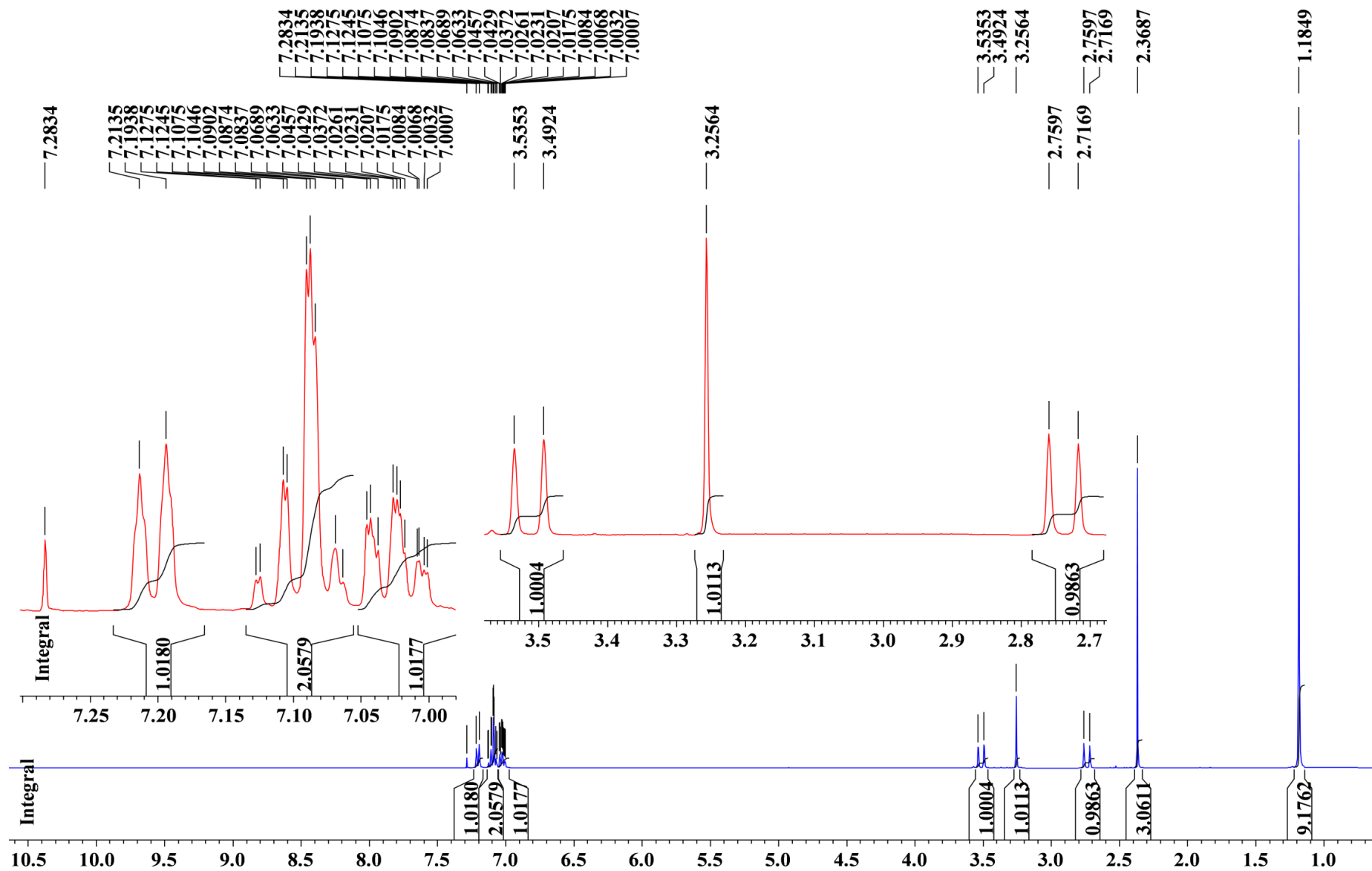


Figure S18. ¹H NMR spectrum (400.0 MHz, CDCl₃, 25°C) of phosphorane (6).

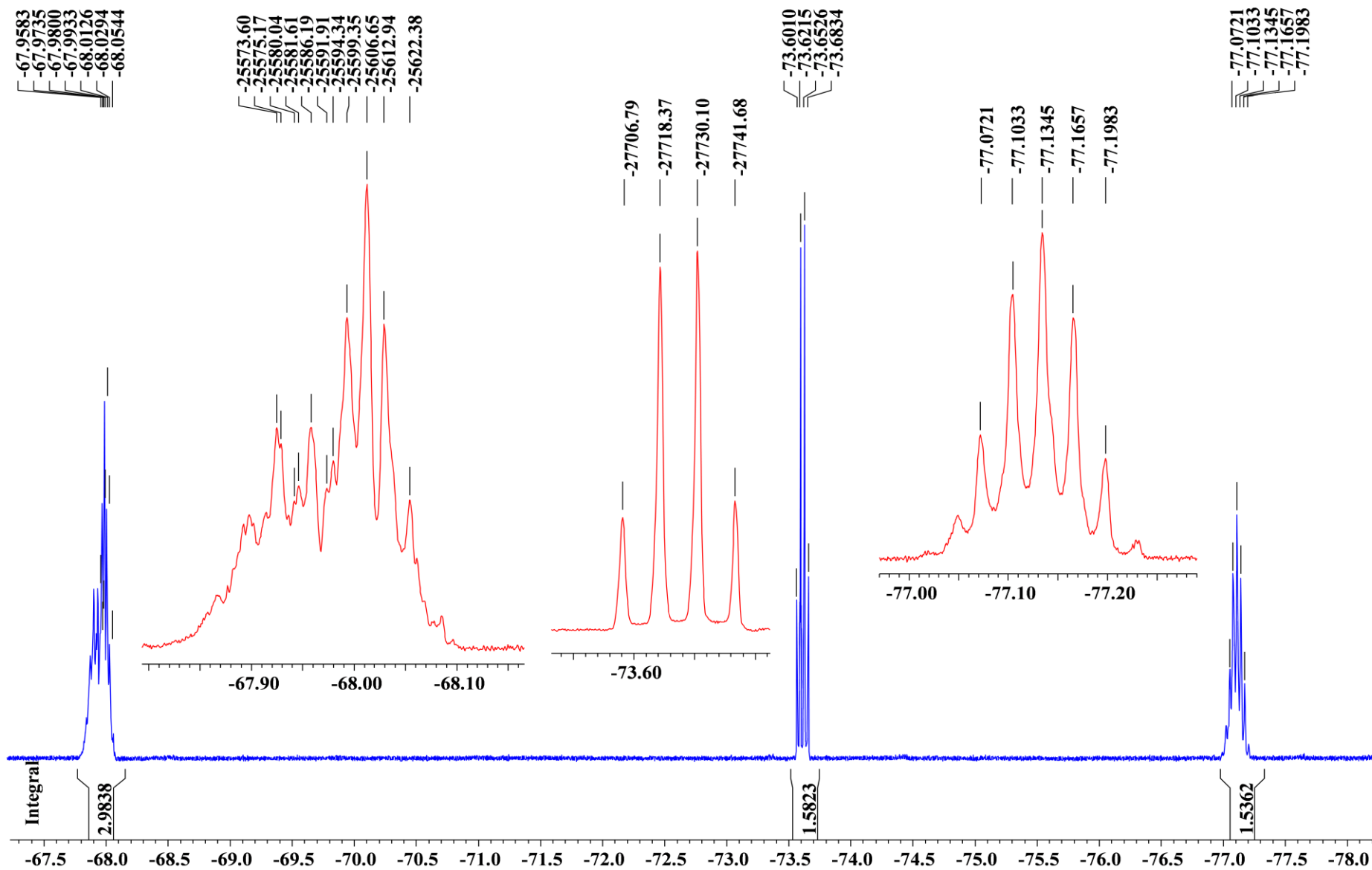


Figure S19. ^{19}F NMR spectrum (386.5 MHz, CDCl_3 , 25°C) of phosphorane (6).

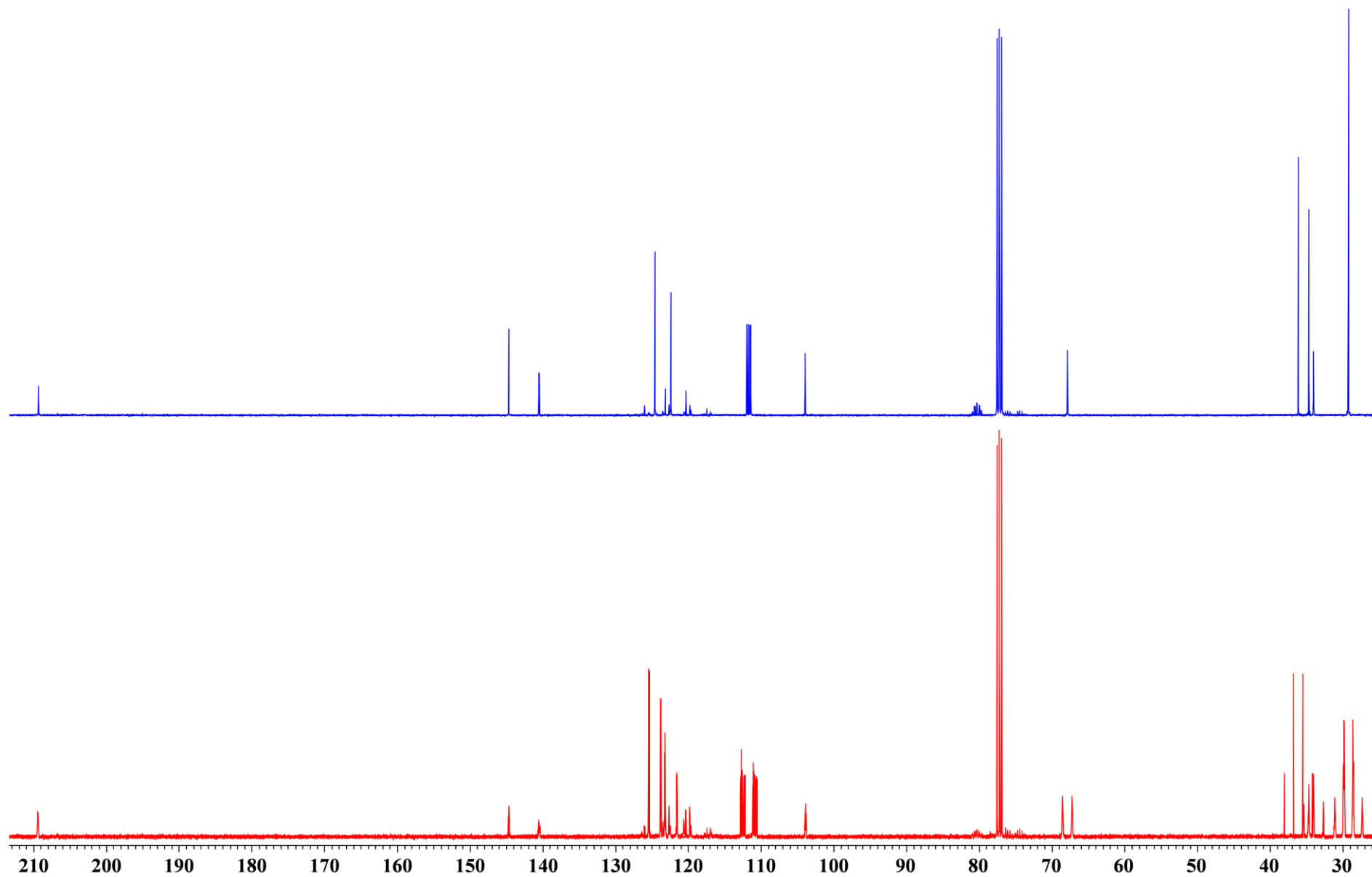


Figure S20. ^{13}C and $^{13}\text{C}\{-^1\text{H}\}$ NMR spectra (100.6 MHz, CDCl_3 , 25°C) of phosphorane (6).

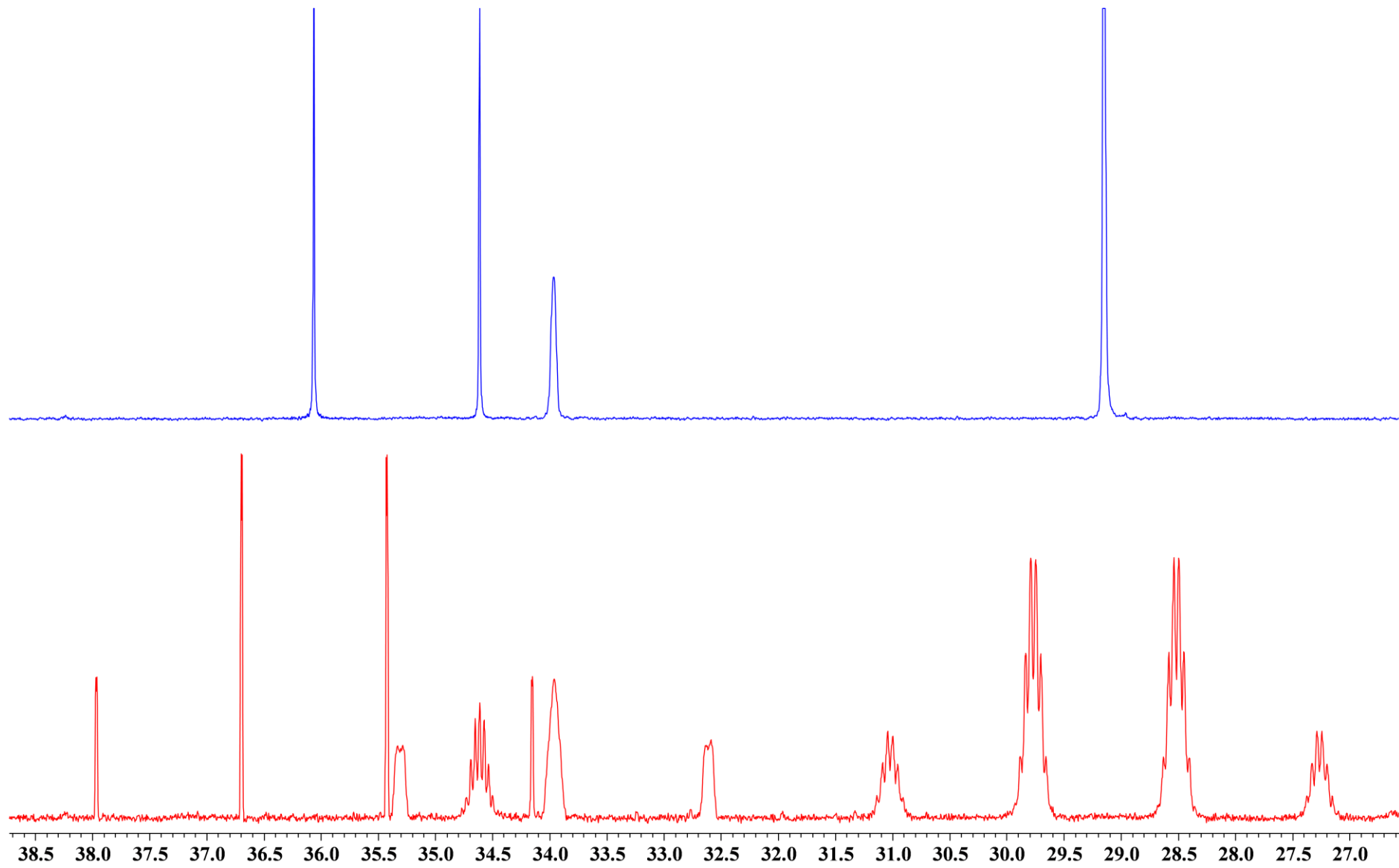


Figure S21. High-field regions of ^{13}C and $^{13}\text{C}\{-^1\text{H}\}$ NMR spectra (100.6 MHz, CDCl_3 , 25°C) of phosphorane (**6**).

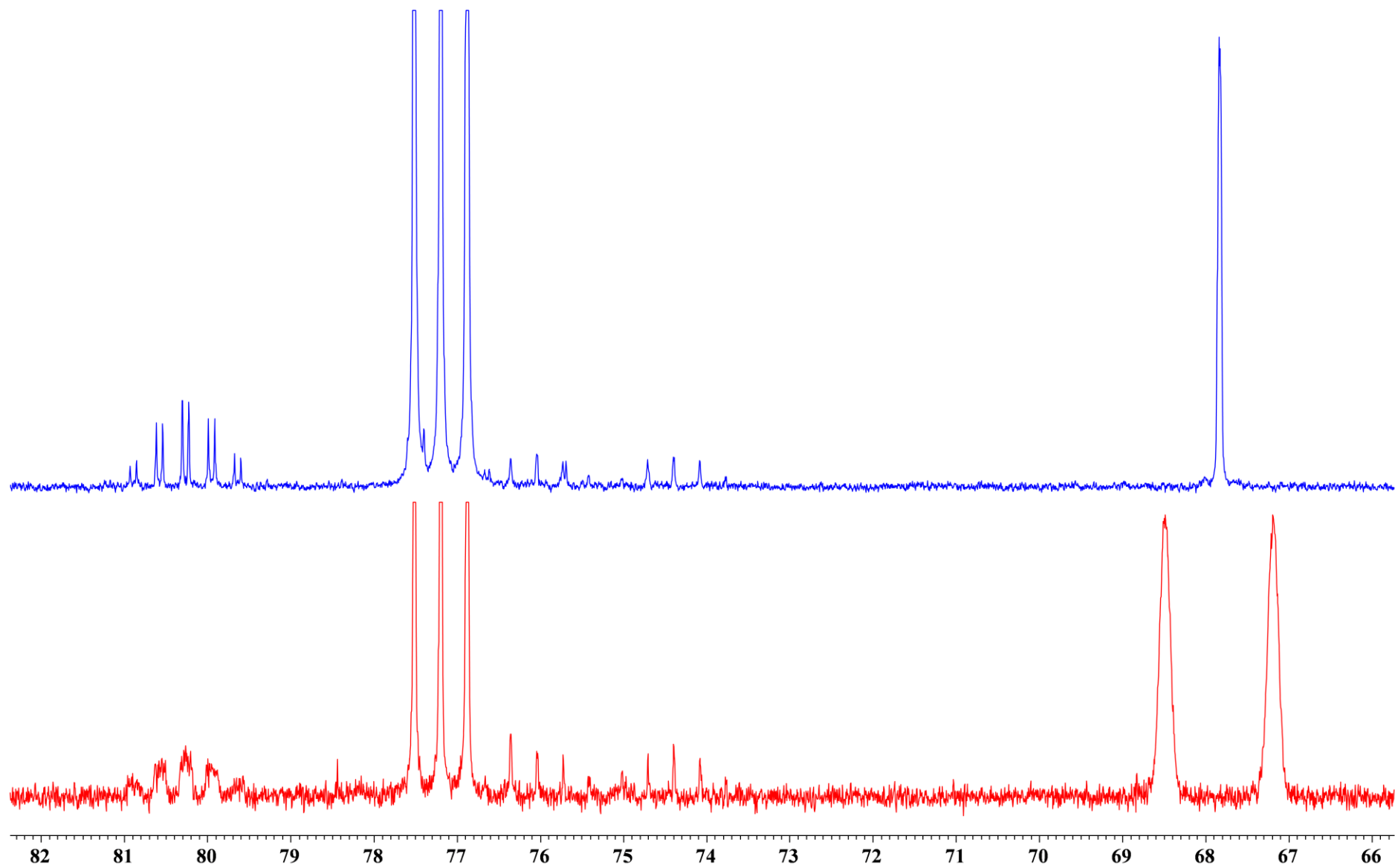


Figure S22. C^3 , C^4 and C^7 region of ^{13}C and $^{13}\text{C}\{-^1\text{H}\}$ NMR spectra (100.6 MHz, CDCl_3 , 25°C) of phosphorane (**6**).

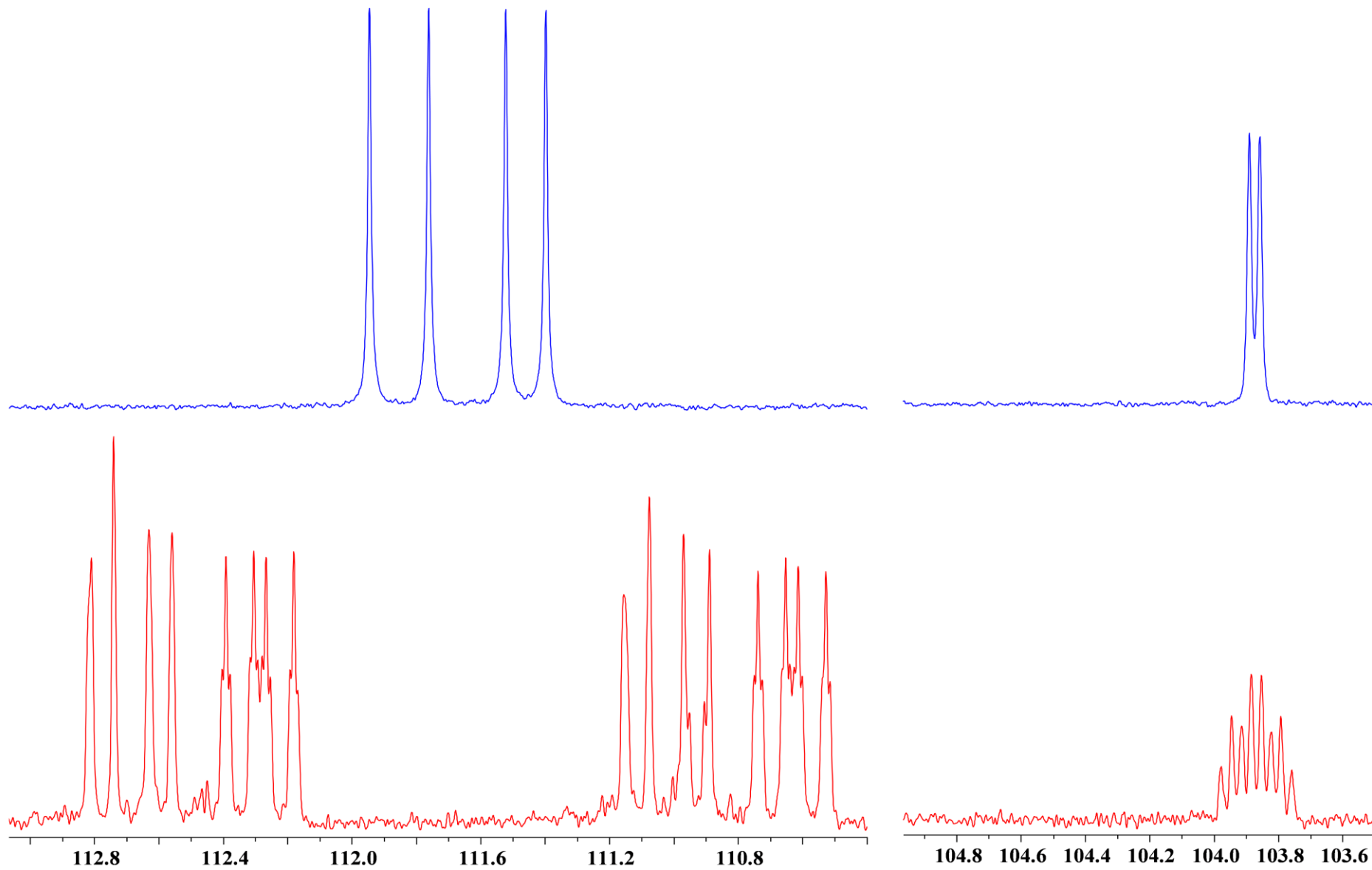


Figure S23. C^9 , C^{12} and C^5 regions of ^{13}C and $^{13}\text{C}\{-^1\text{H}\}$ NMR spectra (100.6 MHz, CDCl_3 , 25°C) of phosphorane (6).

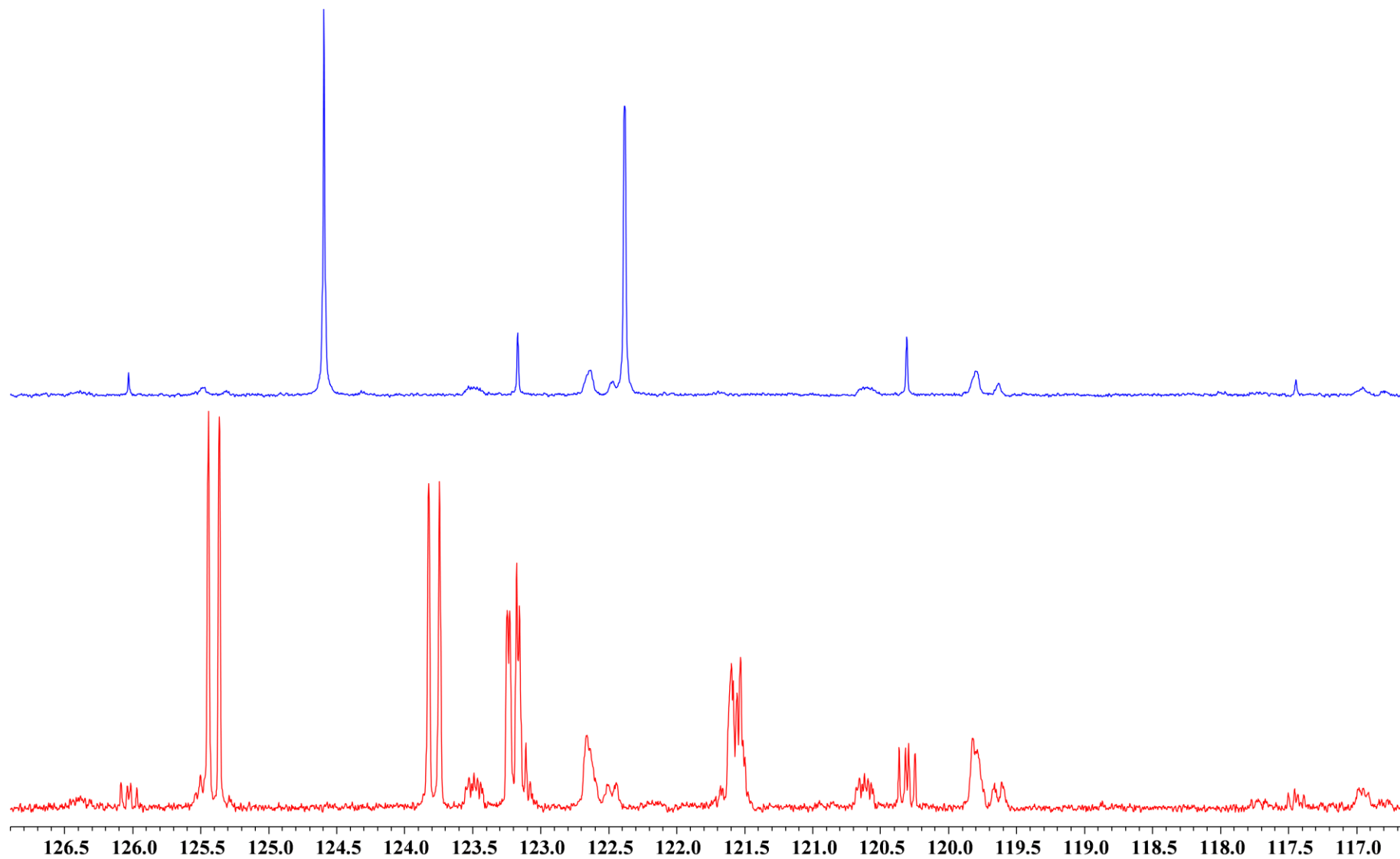


Figure S24. Aromatic carbons and CF_3 -groups region of ^{13}C and $^{13}\text{C}\{-^1\text{H}\}$ NMR spectra (100.6 MHz, CDCl_3 , 25°C) of phosphorane (**6**).

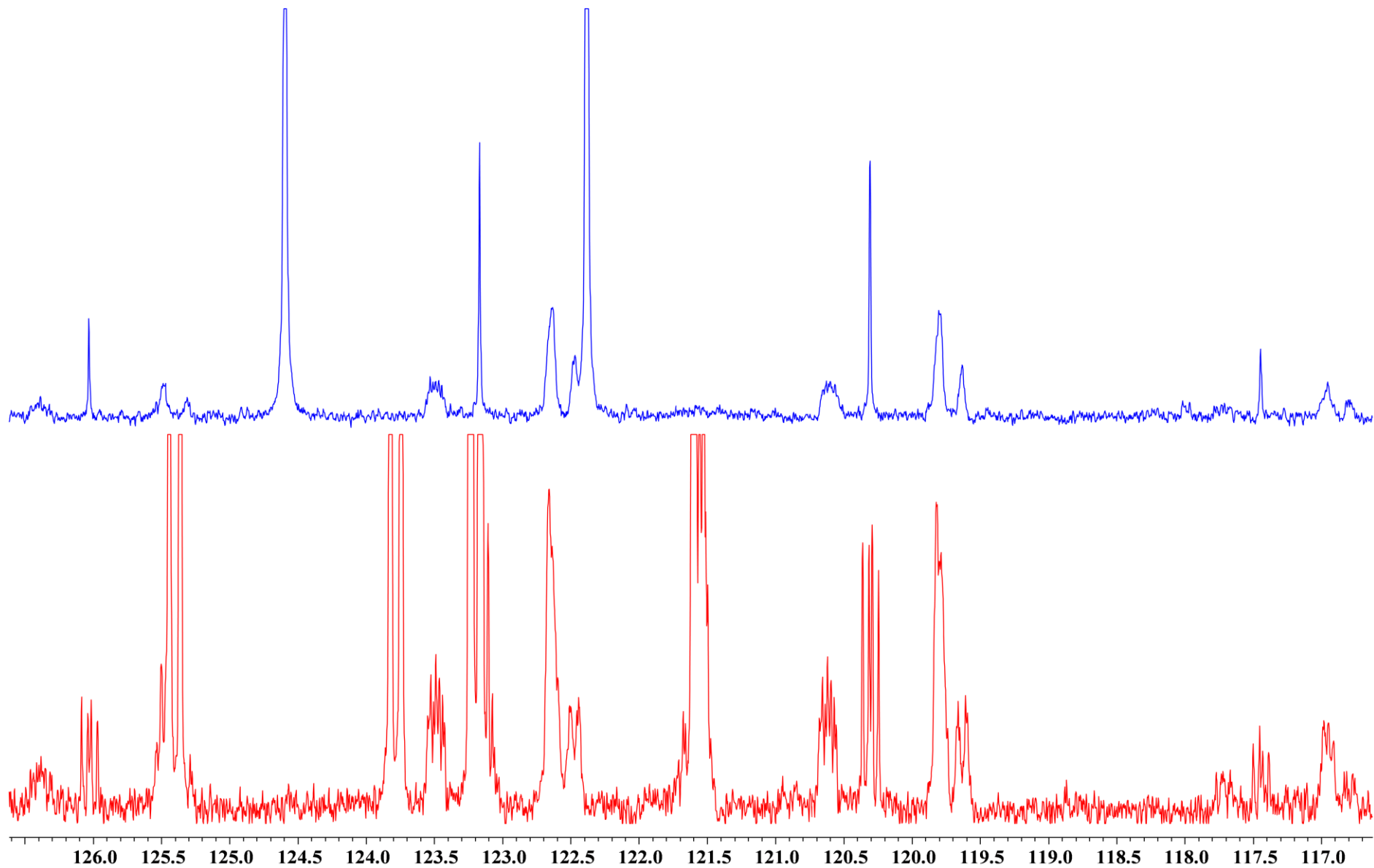


Figure S25. CF₃-groups region of ¹³C and ¹³C-{¹H} NMR spectra (100.6 MHz, CDCl₃, 25°C) of phosphorane (6).

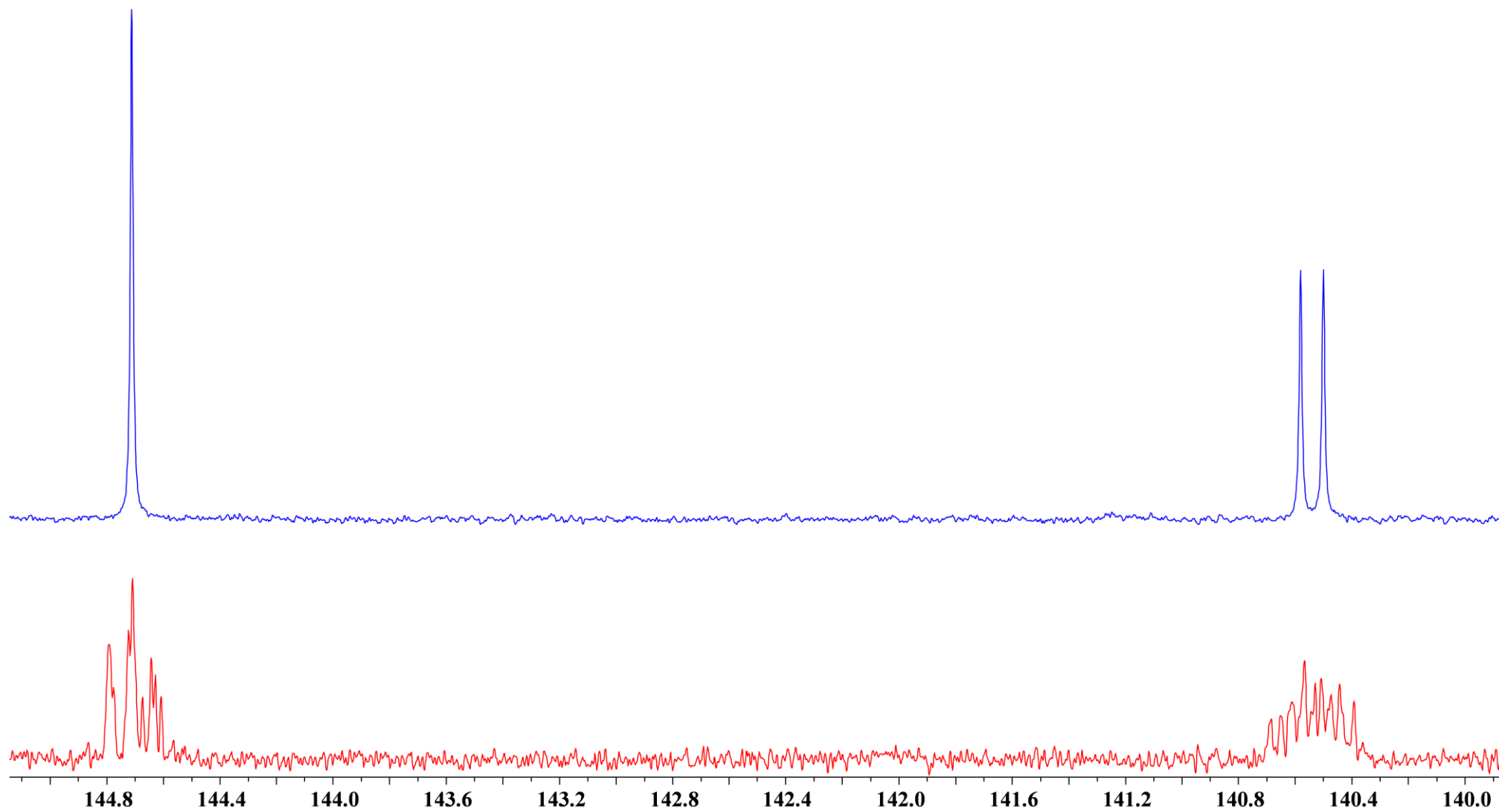


Figure S26. Low-field region of ^{13}C and $^{13}\text{C}\{-^1\text{H}\}$ NMR spectra (100.6 MHz, CDCl_3 , 25°C) of phosphorane (**6**).

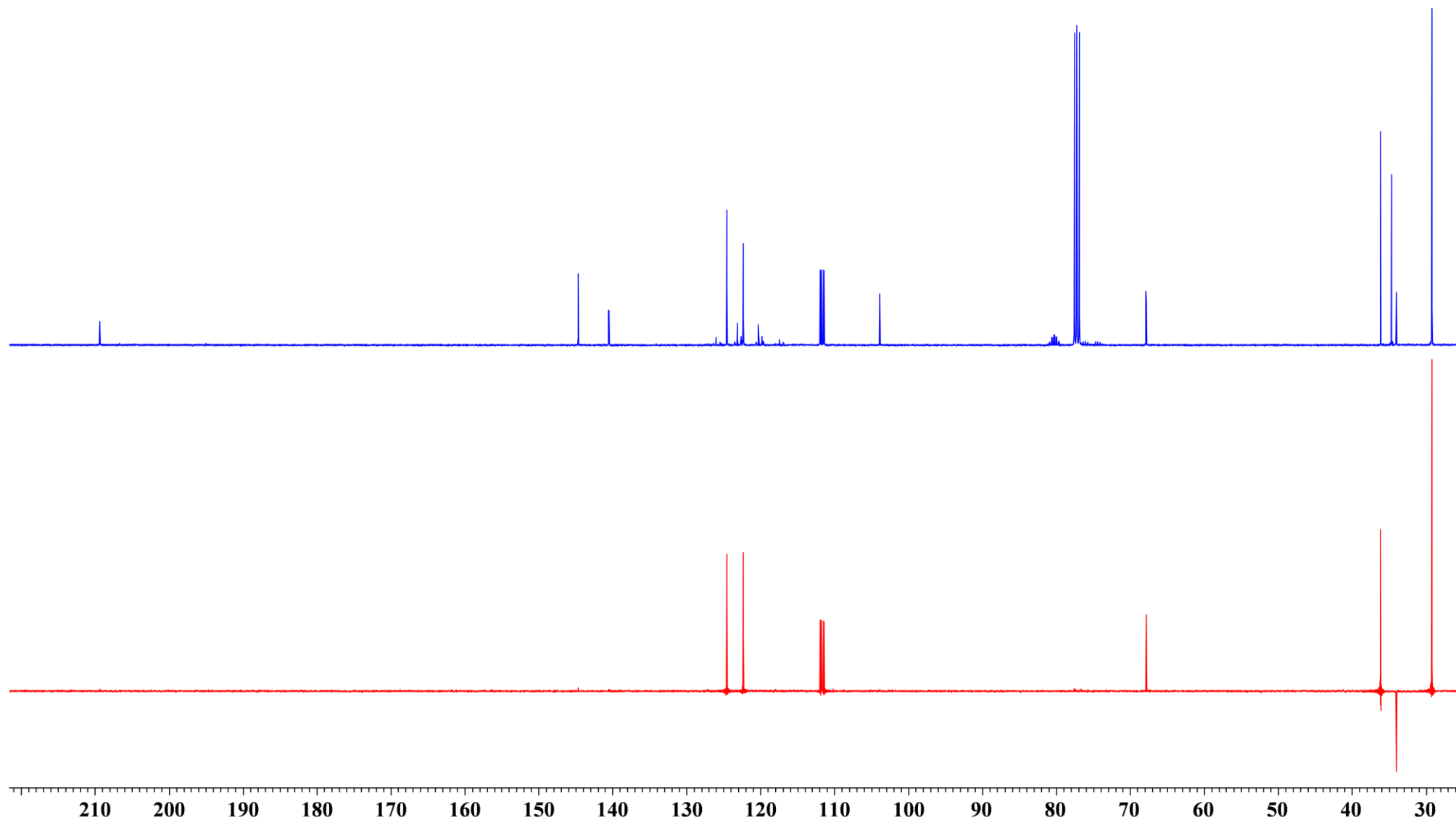


Figure S27. $^{13}\text{C}\{-^1\text{H}\}$ and ^{13}C -dept NMR spectra (100.6 MHz, CDCl_3 , 25°C) of phosphorane (6).

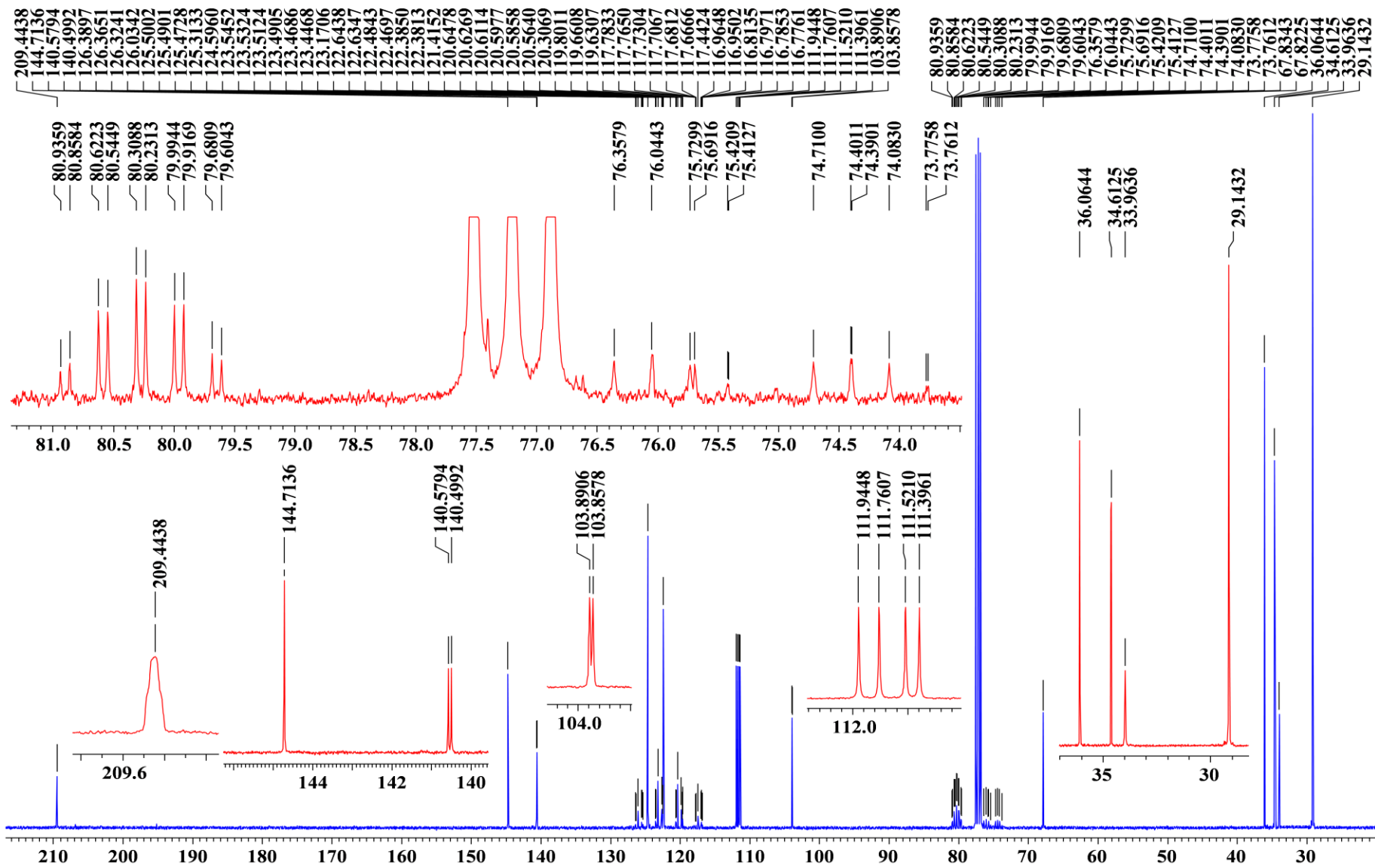


Figure S28. ^{13}C - $\{^1\text{H}\}$ NMR spectrum (100.6 MHz, CDCl_3 , 25°C) of phosphorane (6).

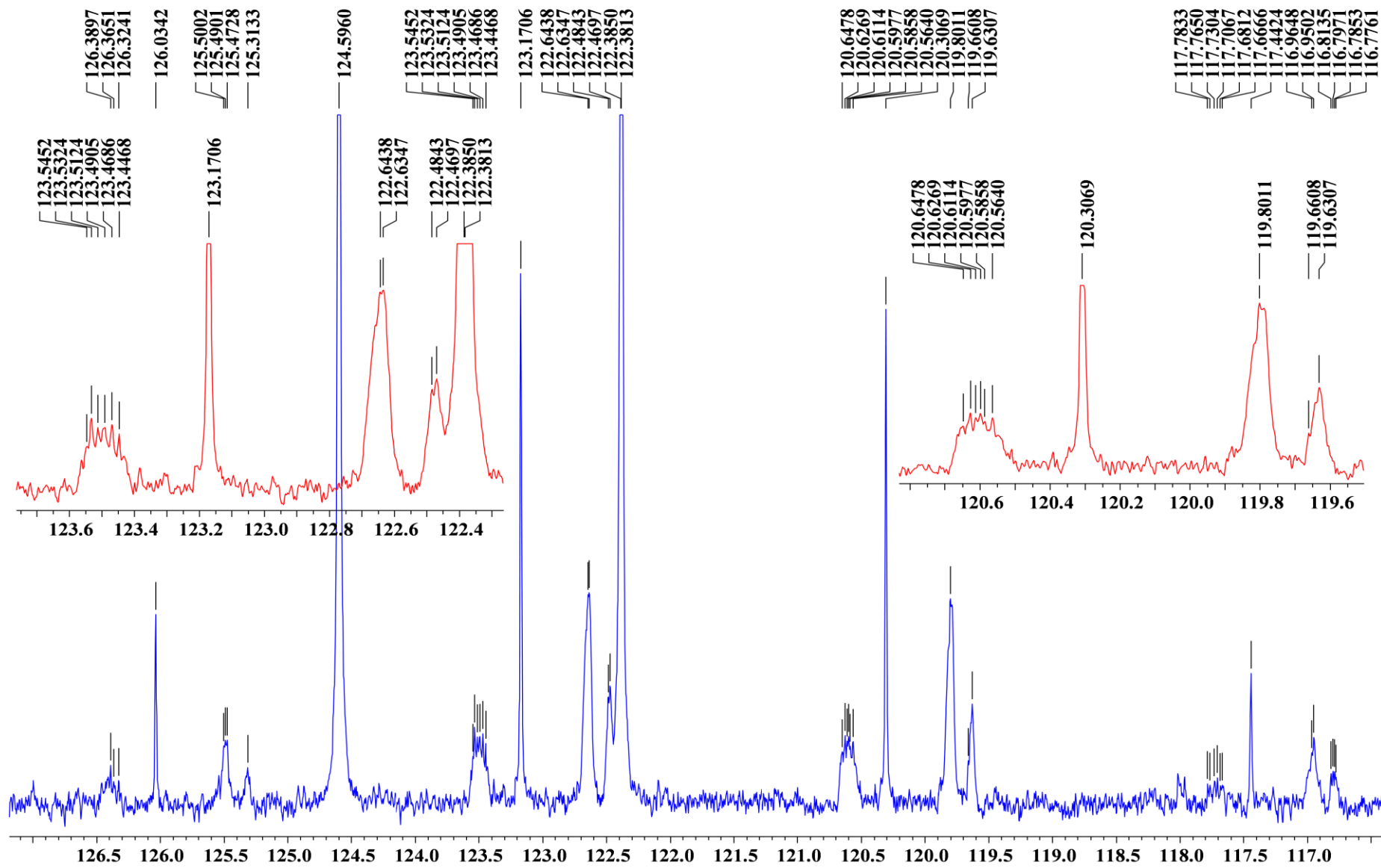


Figure S29. Aromatic carbons and CF₃-groups region of ¹³C-¹H NMR spectrum (100.6 MHz, CDCl₃, 25°C) of phosphorane (6).

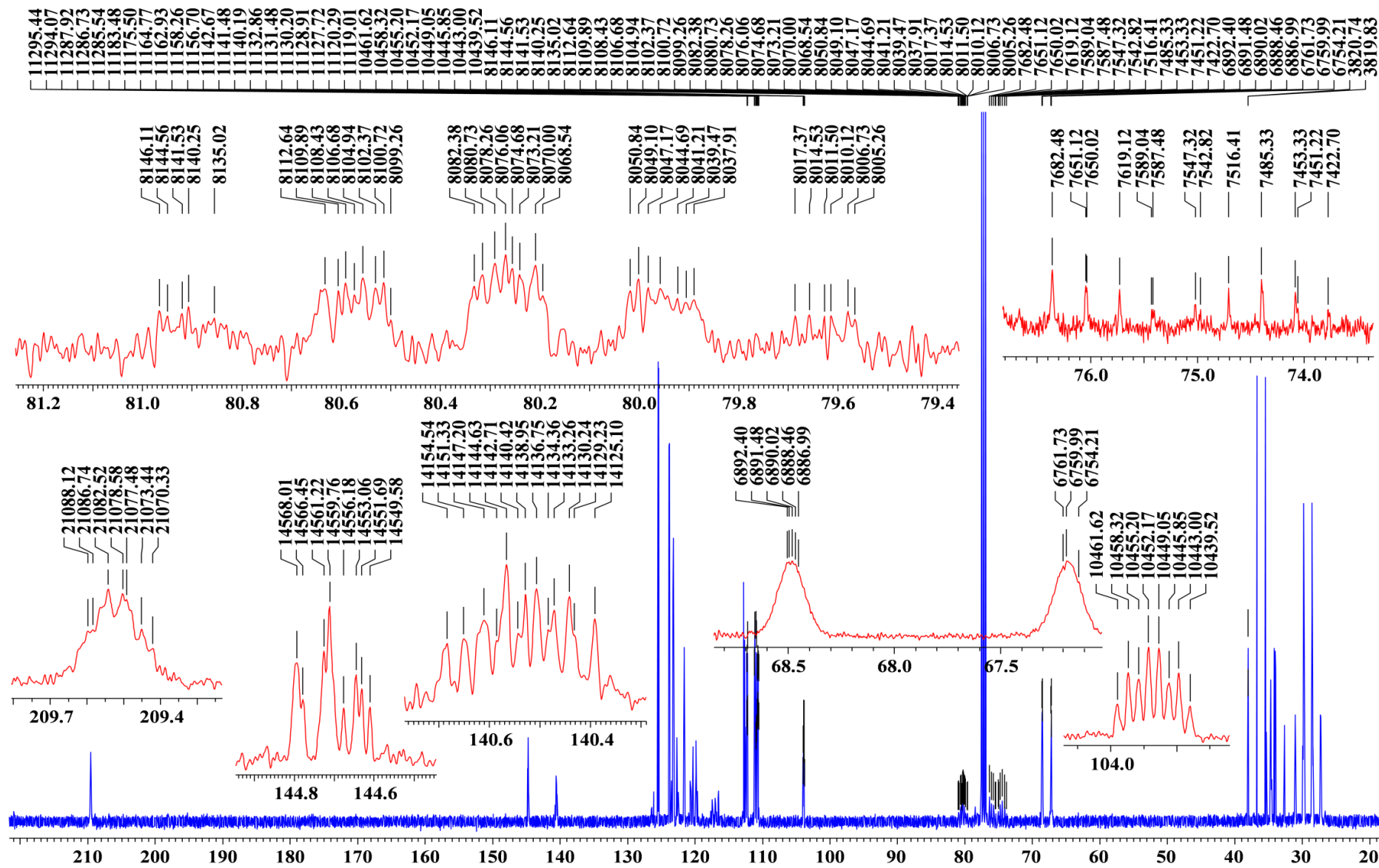


Figure S30. ^{13}C NMR spectrum (100.6 MHz, CDCl_3 , 25°C) of phosphorane (6).

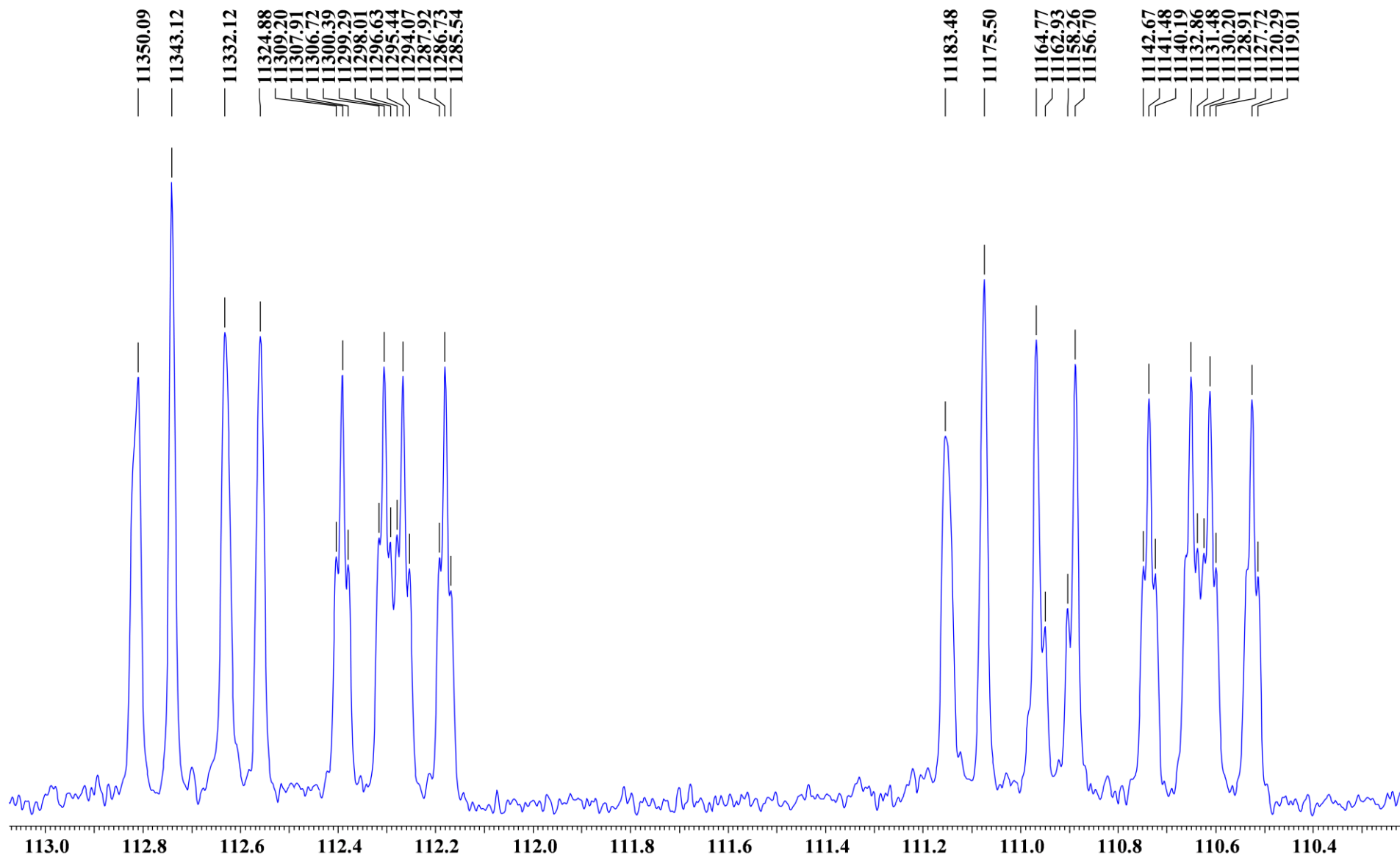


Figure S31. C⁹ and C¹²-atoms region of ¹³C NMR spectrum (100.6 MHz, CDCl₃, 25°C) of phosphorane (6).

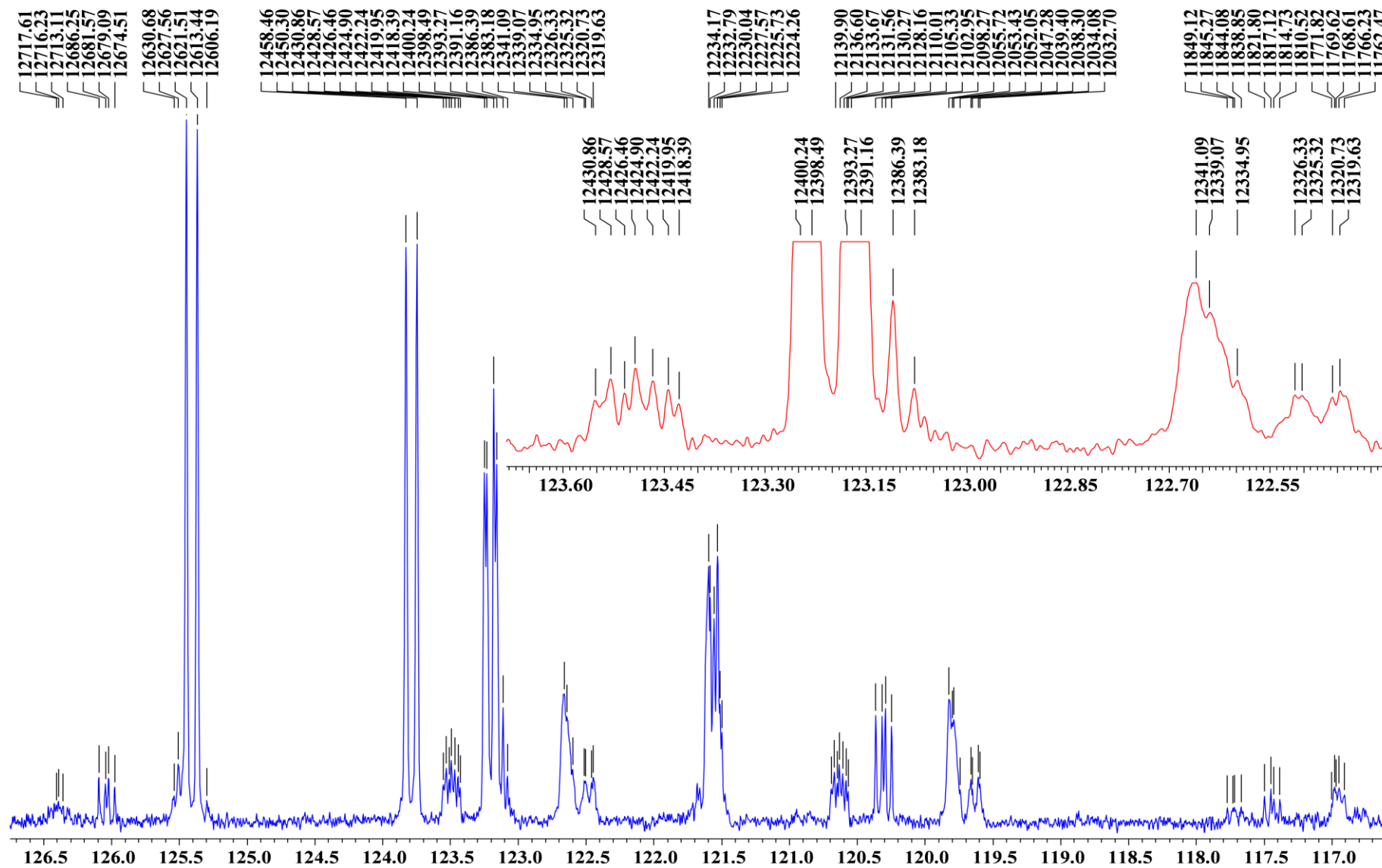


Figure S32. Aromatic carbons and CF_3 -groups region of ^{13}C NMR spectrum (100.6 MHz, CDCl_3 , 25°C) of phosphorane (6).

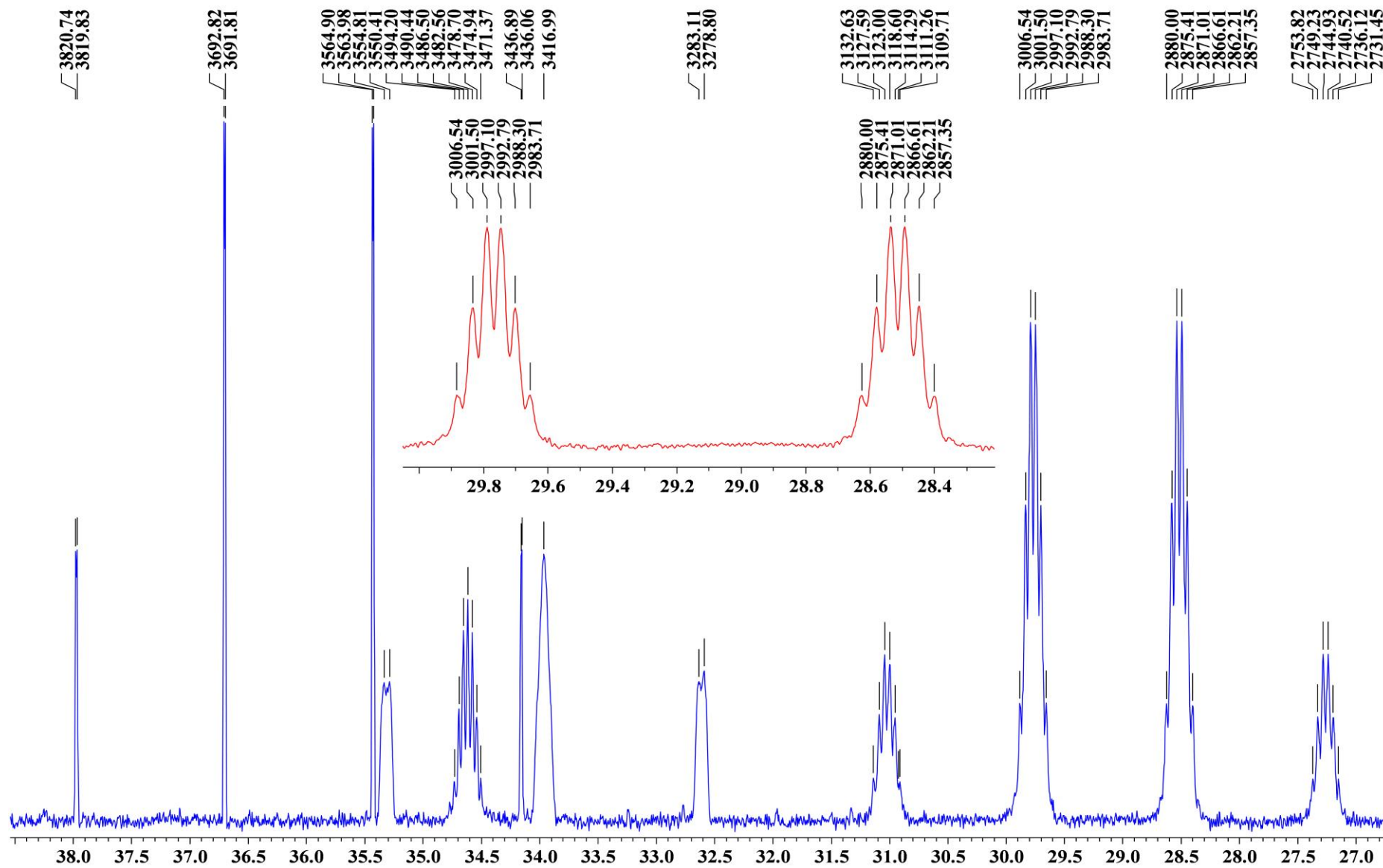


Figure S33. High-field region of ^{13}C NMR spectrum (100.6 MHz, CDCl_3 , 25°C) of phosphorane (6).

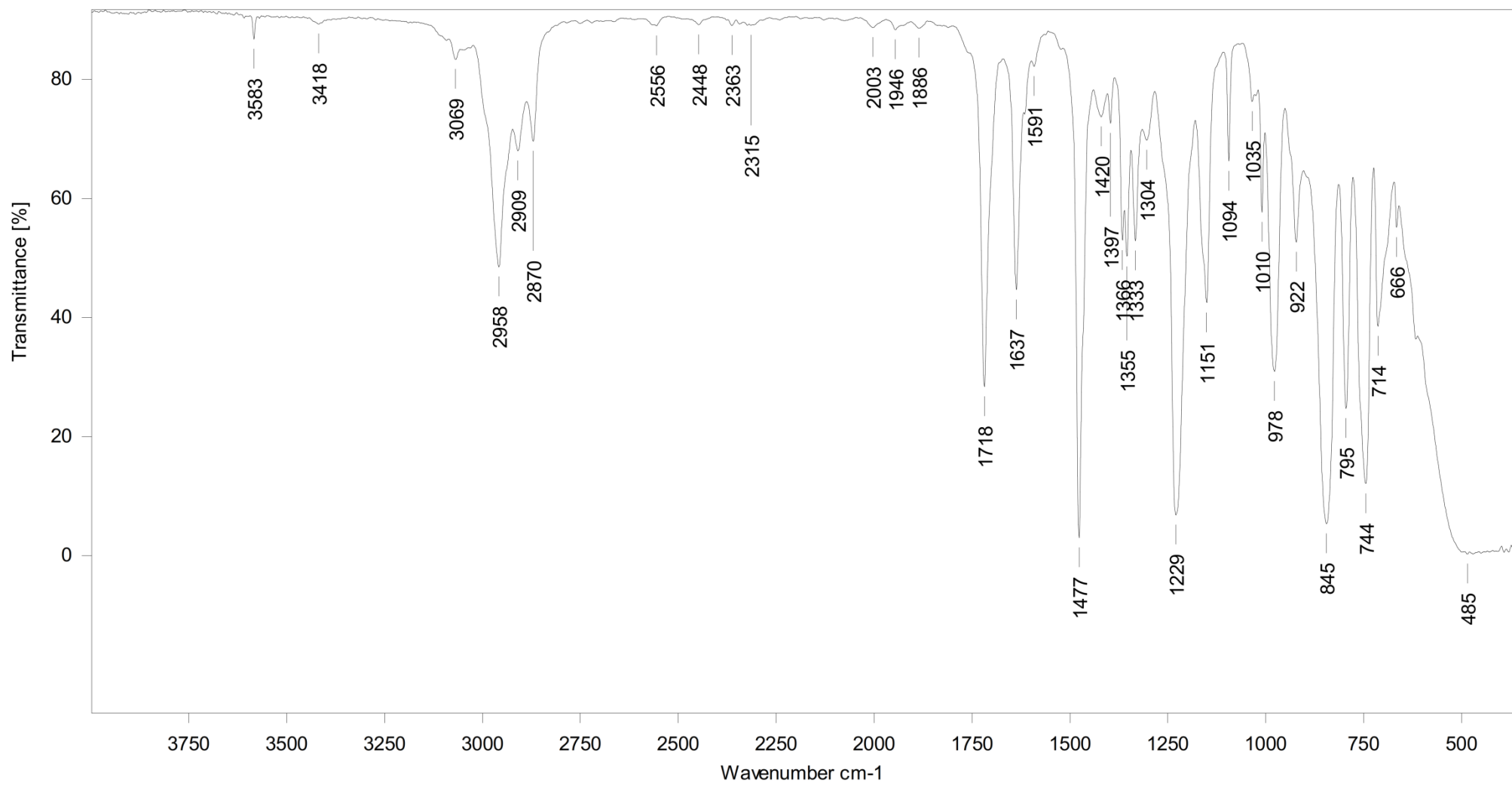


Figure S34. IR Spectrum (Nujol) of phosphole (3).

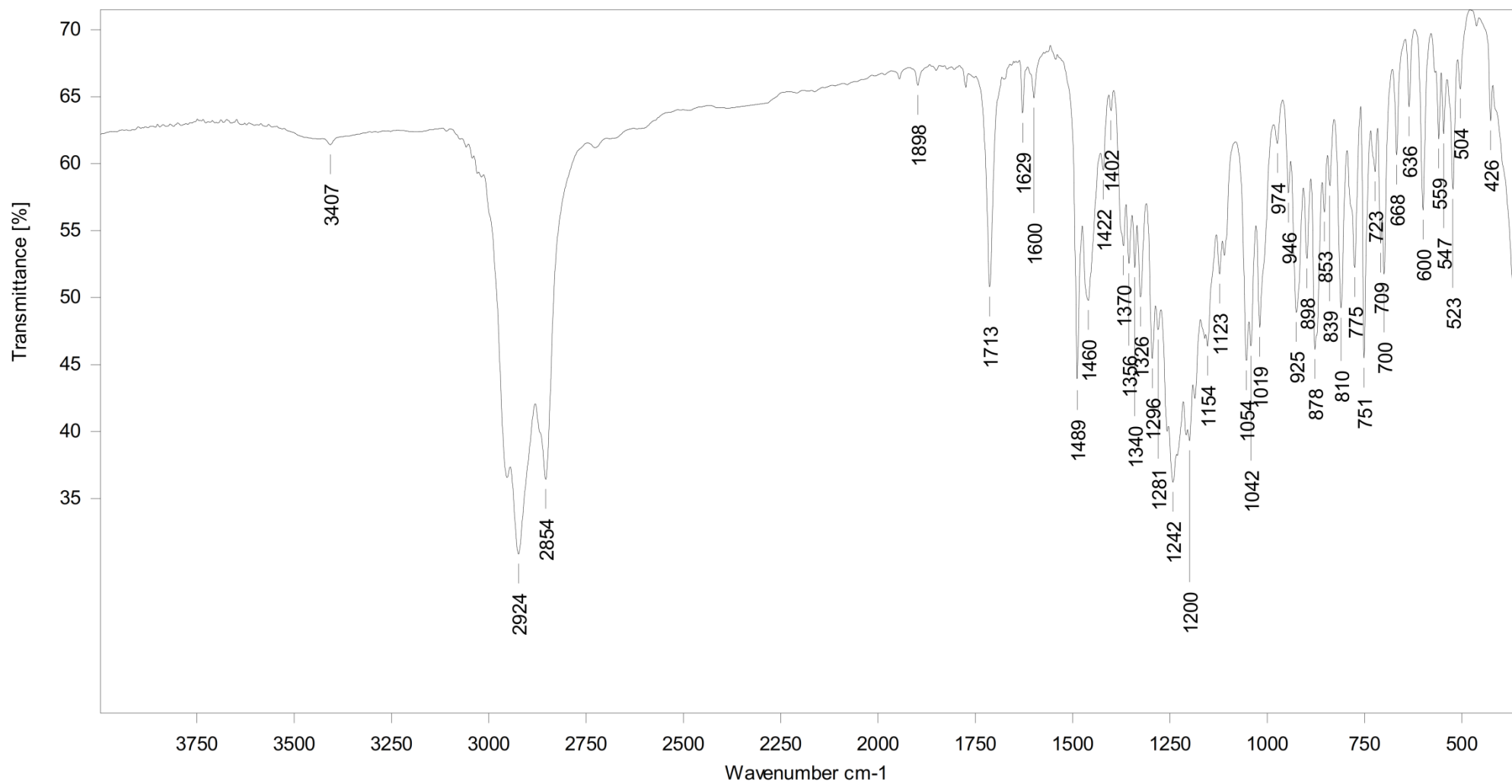


Figure S35. IR Spectrum (Nujol) of phosphorane (**6**).